

Towards a global theory for the high T_c cuprates: Explanation of the puzzling optical properties

J. Ashkenazi*

*Physics Department, University of Miami,
P.O. Box 248046, Coral Gables, FL 33124, U.S.A.*

(Dated: October 3, 2018)

A theory has been worked out for the cuprates, which is based on the major features of their first-principles-derived electronic structure, including the contribution of a large- U band. Within this theory the puzzling physics of the cuprates is shown to be a behavior specific of their structure, within the regime of a Mott transition. The translational symmetry within the CuO_2 planes is disturbed by dynamical stripe-like inhomogeneities, which provide quasi-one-dimensional segments where the large- U scenario of separation between spin and charge is materialized. However, these charge carriers gain itineracy only due to the coupling with electrons in the regions where spin and charge are inseparable. Consequently a two-component scenario is obtained of heavy and light charge carriers, which are coupled through spin carriers. The theory could explain all the anomalous properties of the cuprates that were studied by it, including those observed in transport, tunneling, ARPES, and neutron-scattering results, the pairing mechanism and its symmetry, the observed phase diagram, and the occurrence of intrinsic nanoscale heterogeneity. Here this theory is applied to study a variety of puzzling optical properties of the cuprates, and again provides a natural explanation, for each property tested. This includes “violations” of the f-sum rule, Tanner’s law, Homes’ law, Uemura’s law, the behavior of the n/m^* ratio with doping, the behavior in the heavily underdoped and overdoped regimes, states within the gap and on its edge, the drop in the ab -plane scattering rate below T^* and T_c , the gap-like behavior of the c -direction optical conductivity below T^* , and c -direction collective modes.

PACS numbers: 71.10.Hf, 71.10.Li, 71.10.Pm, 71.30.+h, 74.20.-z, 74.20.Mn, 74.25.Dw, 74.25.Gz, 74.72.-h

I. INTRODUCTION

The unusual physics of the cuprates, and specifically the occurrence of high- T_c superconductivity (SC) in them [1], continues to be one of the forefront problems in physics. Even though numerous mechanisms have been proposed to explain this puzzling system (*e.g.*, Refs. [2–13]), a consensus has not been reached yet. The cuprates, as well as related systems of interest, are characterized by such a complexity that it may make it unrealistic, at present, to predict the different aspects of their behavior by a precisely solvable model or numerical calculations. Their complexity involves single-particle [14–16], many-body [17–19], and lattice effects [20, 21], as well as the occurrence of nanoscale inhomogeneity [22–28].

Even though approximate numerical calculations, and solutions of simple models, have been helpful [17–19, 29–47], an approach incorporating results of different schemes may be necessary for the *global* understanding of the cuprates. In spite that a rigorous analytical or numerical solution of the incorporated scheme, in its globality, is beyond reach at present, it provides an insight to the understanding of the physics of the cuprates, which is missing when models which describe the system partially are applied.

Such an approach, including a minimal framework

within which different aspects of the physics of the cuprates could be described correctly, has been worked out by the author [48–50]. Within this emerging ‘global theory’ of the cuprates (GTC) their puzzling physics, including the occurrence of high- T_c SC, can be understood as the result of a behavior typical of their structure within the regime of a Mott transition [6]. A solution has been studied, corresponding to a state where translational symmetry within the CuO_2 planes is disturbed by dynamical stripe-like inhomogeneities. Signatures of such inhomogeneities have been observed, *e.g.*, in Refs. [23, 26]. They accommodate the competing effects of hopping and antiferromagnetic (AF) exchange on large- U electrons, and their existence had been predicted theoretically [29–32].

These inhomogeneities provide quasi-one-dimensional segments in which the behavior of the electrons is described in terms of separate carriers of charge and spin [3]. Since these carriers are strongly coupled to electrons in the regions where spin and charge are inseparable, a two-component scenario is obtained of heavy and light charge carriers, coupled through spin carriers. The speed of the dynamics of the stripe-like inhomogeneities is self-consistently determined by the width of spin excitations around the AF wave vector $\mathbf{Q} = (\frac{\pi}{a}, \frac{\pi}{a})$. Small-width excitations, and slow dynamics, are obtained in the SC state, and to some degree in the pseudogap (PG) state [49, 50].

This theory was found to provide a highly-plausible explanation to *all* the anomalous properties of the cuprates

*Electronic address: jashkenazi@miami.edu

that were studied by it. This includes the systematic anomalous behavior of the resistivity, Hall constant, and thermoelectric power (TEP) [48], and of spectroscopic anomalies [49, 50]. Also were explained the low- and high-energy spin excitations around \mathbf{Q} , including the neutron-resonance mode [49, 50], and its connection to the peak-dip-hump structure observed in tunneling and ARPES [50]. Pairing was shown [49] to be induced by the energy gain due to the hopping of pair states perpendicular to the stripe-like inhomogeneities. Pairing symmetry was predicted to be of the $d_{x^2-y^2}$ type, but to include features not characteristic of this symmetry [49].

The phase diagram of the cuprates was found [50] to result from an interplay between pairing and coherence within the regime of the Mott transition. Both pairing and coherence are necessary for SC to occur. Coherence without pairing results in a metallic Fermi-liquid (FL) state. Incoherent pairing results in the PG state, consisting of electrons and localized electron pairs. At low temperatures (T), the stripe-like inhomogeneities partially freeze in the PG state into a glassy “checkerboard” structure [27], and the electrons become localized. This results in the opening of localization minigaps on the Fermi surface (FS); they contribute to the PG, and their size determines the lower doping limit of the SC phase. If SC is suppressed, the borderline between the FL and the PG states persists down to $T = 0$, where a metal-insulator-transition (MIT) quantum critical point (QCP) occurs [51, 52].

A nanoscale heterogeneity was predicted [50], especially in the underdoped (UD) regime, consisting of “perfectly” SC regions which become completely paired for $T \rightarrow 0$, and “PG-like” SC regions, where pairing remains partial as in the PG state. A distribution of such regions of different degrees of pairing has been observed by STM [28]. This heterogeneity is expected to be intrinsic, and set in below T_c even in very pure samples. Its scale is larger than that of the dynamical stripe-like inhomogeneities, which are also intrinsic and essential for high- T_c SC [49]. Injection of pairs, similar to the one occurring in p-n junctions in semiconductors, is expected in junctions including slices of a cuprate in the SC state and in the PG state, resulting in the observed “giant proximity effect” (GPE) [53].

Similarly to transport, optical properties detect the electrons *within* the crystal, with no transfer of electrons into, or out of it (as occurs *e.g.* in tunneling or ARPES). Thus, even though their theoretical evaluation involves an integration over the Brillouin zone (BZ), they still could be very sensitive to fine many-body effects. The relevance of optical results to the theoretical predictions of Refs. [48–50] has been mentioned there just in passing. Here it is demonstrated how this GTC naturally explains a variety of optical results (whichever were tested by it), detailed below, part of which have been lacking a satisfactory understanding so far.

The partial Glover–Ferrell–Tinkham sum rule (f-sum rule) [37, 38, 54–56], over the conduction band, is studied.

The GTC is applied to understand observed “violations” of the sum rule through T_c , due to the transfer of spectral weight from energies $\gtrsim 2$ eV to the vicinity of the Fermi level (E_F) [57–60]. Also the optical signatures of c -axis collective modes [56, 61–65] are understood.

The physical interpretation of the optical density to mass (n/m^*) ratio, derived, *e.g.*, through the f-sum rule is clarified. The GTC is shown to explain “Tanner’s law” [66], under which the above ratio is about 4–5 times the contribution to it from the Drude part of the optical conductivity σ , which happens to be just a little greater than the ratio n_s/m^* based on the low- T superfluid density n_s . The approximate factor of four is connected to the periodicity within the stripe-like inhomogeneities. The increase in this factor in the heavily UD regime, as well as the occurrence of a constant effective mass of carriers through the transition to the AF regime [67], are also understood.

The optical quantity $\rho_s = 4\pi e^2 n_s/m^*$ is shown here to be *not* identical with the quantity obtained through the relation $\rho_s = (c/\lambda)^2$ from measurements of the penetration-depth λ by methods like μSR (as has been observed [68]), due to a difference between the many-body effects on them. In the second case the GTC predicts [48–50] a boomerang-type behavior in the overdoped (OD) regime, in agreement with experiment [69]. But, as is shown here, no such behavior is expected for the optical ρ_s , also in agreement with experiment [70].

Within the GTC, the dynamical stripe-like inhomogeneities are intertwined with low-energy spin excitations around \mathbf{Q} (including the resonance mode), which contribute narrow peaks only in the PG and SC states. It is demonstrated here that their optical signatures have been observed [71–75] in these states at energies on the edge of the gap, and within it.

This theory is also shown to explain the different optical signatures of the PG in the c -direction and in the ab -plane. Namely the observation of a depression, within the PG energy range, of the optical conductivity $\sigma(\omega)$, in the c -direction [76, 77], but of the optical scattering rate $1/\tau(\omega)$ in the ab -plane [77, 78].

The sharp drop in this scattering rate below T_c [77, 79] is also predicted by the GTC. The existence of the QCP in the phase diagram [50] results in marginal-Fermi-liquid (MFL) [5] behavior of the scattering rate above T_c , close to the QCP [80], and to critical behavior of optical quantities [81].

“Uemura’s law”, under which $T_c \propto \rho_s$ in the UD regime [82], has been understood [48–50] on the basis of the pairing phase “stiffness” [7]. Also the optically-derived “Homes’ law” [83], under which $\rho_s \simeq 35\sigma(T_c)T_c$, for cuprates in the entire doping (x) regime, both in the ab -plane, and in the c -direction, and also for low- T_c SC’s in the dirty limit, is shown to be consistent with the GTC. The validity of this law in the cuprates is related to the existence of quantum criticality there [84].

Even though Homes’ law is an approximate one (presented in a log–log scale), its coexistence with Uemura’s

law in the UD regime implies that the DC conductivity at T_c varies considerably less with x (in this regime) than its variation at high temperatures [85]. This behavior is predicted by the GTC as well, and also are understood apparent deviations from Uemura’s law in the heavily UD regime [86].

II. SCHEME OF THE THEORY [48–50]

A. Large- U -limit formalism

Ab-initio calculations [15] in the cuprates indicate that the electrons in the vicinity of E_F could be analyzed in terms of a band (corresponding dominantly to copper and oxygen orbitals within the CuO_2 planes) for which large- U -limit approximations are adequate, which is somewhat hybridized to other bands for which small- U -limit approximations may be suitable. A perturbation expansion in U is inadequate for the large- U orbitals, and they are treated by the auxiliary-particles approach [87]. Thus, within the CuO_2 planes, a large- U electron in site i and spin σ (which is assigned numbers ± 1 , corresponding to \uparrow and \downarrow , respectively) is created by $d_{i\sigma}^\dagger = e_i^\dagger s_{i,-\sigma}$, if it is in the “upper-Hubbard-band”, and by $d_{i\sigma}^\dagger = \sigma s_{i\sigma}^\dagger h_i$, if it is in a Zhang-Rice-type “lower-Hubbard-band”.

Here e_i^\dagger and h_i^\dagger are creation operators of “excessions” and “holons”, and $s_{i\sigma}^\dagger$ are creation operators of “spinons”. If either the excessions, or the holons are ignored, than the large- U band could be treated within the t - t' - J (or t - t' - t'' - J) model. The auxiliary-particle approach is applied here using the “slave fermion” method [87], within which the holons/excessions are fermions and the spinons are bosons. This method had been successful treating antiferromagnetic (AF) systems, and implies taking good account of the effect of AF correlations. For rigorous treatment, one should in principle impose in each site the constraint: $e_i^\dagger e_i + h_i^\dagger h_i + \sum_\sigma s_{i\sigma}^\dagger s_{i\sigma} = 1$.

In order to treat this constraint properly, an auxiliary Hilbert space is introduced within which a chemical-potential-like Lagrange multiplier is used to impose the constraint on the average. But since the physical observables are projected into the physical space as combinations of Green’s functions, whose time evolution is determined by the Hamiltonian which obeys the constraint rigorously, it is expected that it would not be violated as long as justifiable approximations were used.

The dynamics of the stripe-like inhomogeneities is approached adiabatically, treating them statically with respect to the electrons dynamics. The striped structure [23] consists of narrow charged stripes forming antiphase domain walls between wider AF stripes. Since the spin-charge separation approximation (under which two-auxiliary-particle spinon-holon/excession Green’s functions are decoupled into single-auxiliary-particle Green’s functions) is valid in one-dimension, it is justified to assume the existence of effective spinless charge carriers

within the narrow charged stripes, but not within the whole CuO_2 plane (as is assumed in RVB theory [3]).

B. “Bare” auxiliary particles

The spinons are diagonalized by applying the Bogoliubov transformation for bosons [88]: $s_\sigma(\mathbf{k}) = \cosh(\xi_{\sigma\mathbf{k}})\zeta_\sigma(\mathbf{k}) + \sinh(\xi_{\sigma\mathbf{k}})\zeta_{-\sigma}^\dagger(-\mathbf{k})$. Spinon states, created by $\zeta_\sigma^\dagger(\mathbf{k})$, have bare energies $\epsilon^\zeta(\mathbf{k})$ with a V-shape zero minimum at $\mathbf{k} = \mathbf{k}_0$. Bose condensation results in an AF order of wave vector $\mathbf{Q} = 2\mathbf{k}_0$. Within the lattice BZ there are four inequivalent possibilities for \mathbf{k}_0 : $\pm(\frac{\pi}{2a}, \frac{\pi}{2a})$ and $\pm(\frac{\pi}{2a}, -\frac{\pi}{2a})$, thus introducing a broken symmetry. One has [88]:

$$\begin{aligned} \cosh(\xi_{\mathbf{k}}) &\rightarrow \begin{cases} +\infty, & \text{for } \mathbf{k} \rightarrow \mathbf{k}_0, \\ 1, & \text{for } \mathbf{k} \text{ far from } \mathbf{k}_0, \end{cases} \\ \sinh(\xi_{\mathbf{k}}) &\rightarrow \begin{cases} -\cosh(\xi_{\mathbf{k}}), & \text{for } \mathbf{k} \rightarrow \mathbf{k}_0, \\ 0, & \text{for } \mathbf{k} \text{ far from } \mathbf{k}_0. \end{cases} \end{aligned} \quad (1)$$

Holons (excessions) within the charged stripes are referred to as “stripions”; they carry charge $-e$ but no spin, and are created by fermion operators $p_\mu^\dagger(\mathbf{k})$. A starting point of localized stripion states is assumed, due to the fatal effect of imperfections in the striped structure on itineracy in one dimension. This assumption is supported by the atomic-scale structure observed recently by STM [27], which is consistent with a fluctuating domino-type two-dimensional arrangement of stripe-like inhomogeneities. Such a two-dimensional arrangement has been predicted by the author [49]. The \mathbf{k} wave vectors of the stripion states present \mathbf{k} -symmetrized combinations of localized states to be treated in a perturbation expansion when coupling to the other fields is considered.

Away from the charged stripes, creation operators of approximate fermion basis states of spinon-holon and spinon-excession pairs are constructed [48, 49]. Together with the small- U states they form, within the auxiliary space, a basis to “quasi-electron” (QE) states, carrying charge $-e$ and spin $\frac{1}{2}$, and created by $q_{i\sigma}^\dagger(\mathbf{k})$. The bare QE energies $\epsilon_i^q(\mathbf{k})$ form quasi-continuous ranges of bands within the BZ.

Atomic doping in the cuprates is taking place in interplanar layers (such as in the chains in YBCO) between CuO_2 planes, and orbitals of the doped atoms contribute states close to E_F . These states hybridize with the QE bands, and provide charge transfer to the planes with doping. The QE bands are spanned between the upper and lower Hubbard bands and the vicinity of E_F , with more holon-based states closer to the lower Hubbard band (relevant mainly for “p-type” cuprates), and more excession-based states closer to the upper Hubbard band (relevant mainly for “n-type” cuprates). As the doping level x is increasing, more QE states are moving from the Hubbard bands to the vicinity of E_F , and the

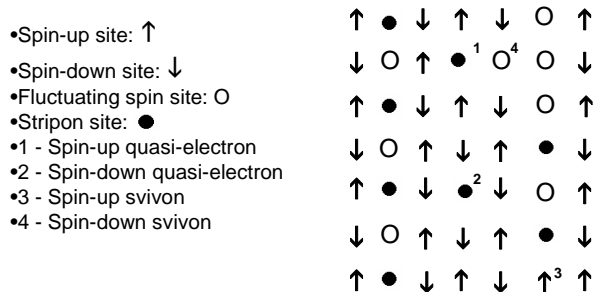


FIG. 1: An adiabatic “snapshot” of a stripe-like inhomogeneity, and the physical signature of the bare auxiliary particles, within a CuO_2 plane.

system is moving from the insulating to the metallic side of the Mott transition regime.

As was mentioned above, the treatment of the constraint, within the auxiliary space, introduces an additional chemical-potential-like Lagrange multiplier. Since the stripions carry only charge, while the QE’s carry both charge and spin, their treatment involves two “chemical potentials”, μ^q and μ^p (corresponding to QE’s and stripions, respectively) whose values are determined by the correct charge, and averaged constraint.

Hopping and hybridization terms introduce strong coupling between the QE, stripion, and spinon fields, which is expressed by a Hamiltonian term of the form (for p-type cuprates):

$$\begin{aligned} \mathcal{H}' = & \frac{1}{\sqrt{N}} \sum_{\lambda\mu\sigma} \sum_{\mathbf{k}, \mathbf{k}'} \{ \sigma \epsilon_{\lambda\mu}^{qp}(\sigma\mathbf{k}, \sigma\mathbf{k}') q_{l\sigma}^\dagger(\mathbf{k}) p_\mu(\mathbf{k}') \\ & \times [\cosh(\xi_{\lambda,\sigma(\mathbf{k}-\mathbf{k}')}) \zeta_{\lambda\sigma}(\mathbf{k}-\mathbf{k}') \\ & + \sinh(\xi_{\lambda,\sigma(\mathbf{k}-\mathbf{k}')}) \zeta_{\lambda,-\sigma}^\dagger(\mathbf{k}'-\mathbf{k}) + h.c. \}, \quad (2) \end{aligned}$$

introducing a vertex between their propagators [89].

The stripe-like inhomogeneities are strongly coupled to the lattice [22], and it is the presence of stripions which creates the charged stripes within them. Also the matrix elements in \mathcal{H}' , are sensitive to the atomic positions [15]. Consequently [50], the spinons are renormalized, being “dressed” by phonons, and thus carry some lattice distortion (but no charge) in addition to spin $\frac{1}{2}$. Such phonon-dressed spinons are referred to as “svivons”, and they replace the spinons in the \mathcal{H}' vertex. This results in strong coupling between electronic spin excitations and Cu–O optical phonon modes [20], and the existence of an anomalous isotope effect [21]. The effect of spin-lattice coupling has been studied by Eremin *et al.* [44].

The physical signature of the auxiliary fields, considering only the large- U band, within the $t-t'-J$ model, is demonstrated in Fig. 1. An adiabatic “snapshot” of a section of a CuO_2 plane, including a stripe-like inhomogeneity, is shown. Within the adiabatic time scale a site is “spinless” either if it is “charged”, removing the spinned electron/hole on it (as in “stripion sites” in Fig. 1), or if the spin is fluctuating on a shorter time scale (due

to, *e.g.*, being in a singlet spin pair). In this description, a site (bare) stripion excitation represents a transition between these two types of a spinless site within the charged stripes, a site (bare) svivon excitation represents a transition between a spinned site and a fluctuating-spin spinless site, and a site (bare) QE excitation represents a transition between a spinned site and a charged spinless site within the AF stripes.

C. Renormalized auxiliary particles

The \mathcal{H}' vertex introduces self-energy corrections to the QE, stripion, and svivon fields [89]. Since the renormalized stripion bandwidth is considerably smaller than the QE and svivon bandwidths, a phase-space argument could be used, as in the Migdal theorem, to ignore vertex corrections. Self-consistent expressions were derived [48, 49] for the self-energy corrections, and spectral functions A^q , A^p , and A^ζ , for the QE, stripion, and svivon fields, respectively. The auxiliary-particle energies ϵ are renormalized to: $\bar{\epsilon} = \epsilon + \Re\Sigma(\bar{\epsilon})$, where Σ is the self energy. Due to the quasi-continuous range of QE bands, the bandwidth renormalization is particularly strong for the stripion energies, resulting in a very small bandwidth, and limited itineracy due to hopping via intermediary QE–svivon states.

The small stripion bandwidth introduces [48, 49] a low-energy scale of ~ 0.02 eV, and an apparent “zero-energy” non-analytic behavior of the QE and svivon self energies within a higher energy range (analyticity is restored in the low-energy range). This behavior results in QE and svivon scattering rates with a term $\sim \omega$, as in the MFL approach [5], but also with a constant term, resulting in a logarithmic singularity in $\Re\Sigma(\omega)$ at $\omega = 0$ (which is truncated by analyticity in the low-energy range). Consequently the QE self-energy has a kink-like behavior of the renormalized QE energies $\bar{\epsilon}^q$ around zero energy [49]. A typical renormalization of the svivon energies, around the V-shape zero minimum of ϵ^ζ at \mathbf{k}_0 , is shown in Fig. 2, where the major effect is due to the truncated logarithmic singularity in the svivon self energy. The svivon spectral functions $A^\zeta(\omega)$ vary continuously around $\omega = 0$, being positive for $\omega > 0$ and negative for $\omega < 0$.

The renormalization of the svivon energies changes the physical signature of their Bose condensation from an AF order to the observed stripe-like inhomogeneities (including both their spin and lattice aspects). The structure of A^ζ and $\bar{\epsilon}^\zeta$ around the minimum at \mathbf{k}_0 (see Fig. 2) determines the structure of the inhomogeneities. Striped structure of the type shown in Fig. 1 results from a direction-dependent slope of $\bar{\epsilon}^\zeta(\mathbf{k})$ at small negative energies. The speed of the dynamics of these inhomogeneities depends on the linewidth of $\bar{\epsilon}^\zeta$ at small negative energies, which is large, unless the system is in a pairing state (thus the SC or PG state), where svivon scattering at such energies is suppressed due to the gap [49] (see below). Consequently, the dynamics of the stripe-like inhomogeneities

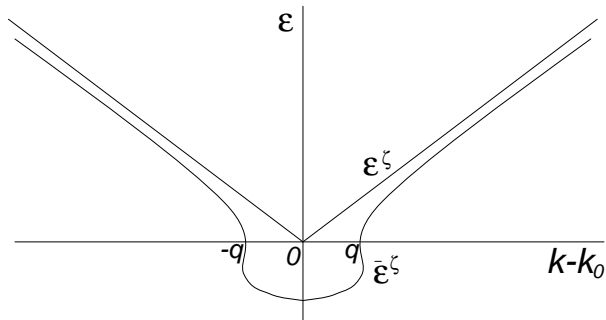


FIG. 2: A typical self-energy renormalization of the svivon energies around the minimum at \mathbf{k}_0 .

becomes sufficiently slow for them to be detected only in a pairing state, in agreement with experiment.

For the renormalized svivons, $\cosh(\xi_{\mathbf{k}})$ and $\sinh(\xi_{\mathbf{k}})$ do not diverge at \mathbf{k}_0 , as in Eq. (1). But still the values of both of them are large in the negative- $\bar{\epsilon}^{\zeta}(\mathbf{k})$ region around this point (see Fig. 2), and thus this region contributes significantly to processes involving svivons. By Eq. (2), the coupling between QE's, stripons, and svivons of this region, are particularly strong when $\bar{\epsilon}^{\eta} \simeq \bar{\epsilon}^{\rho} \pm \bar{\epsilon}^{\zeta}$. On the other hand, a relatively smaller contribution is obtained to such processes from the positive- $\bar{\epsilon}^{\zeta}(\mathbf{k})$ regions, especially when they are sufficiently away from \mathbf{k}_0 , where by Eq. (1) $\cosh(\xi_{\mathbf{k}}) \simeq 1$, and $\sinh(\xi_{\mathbf{k}}) \simeq 0$.

Since the stripons are based on states in the charged stripe-like inhomogeneities, which occupy about a quarter of the CuO_2 plane [23] (see Fig. 1), the number of stripon states is about a quarter of the number of states in the BZ. The \mathbf{k} values mostly contributing to these states reflect, on one hand, the structure of the stripe-like inhomogeneities, and on the other hand, the minimization of free energy, achieved when they reside mainly at BZ areas where their coupling to the QE's and svivons, is optimal. This occurs [49] for stripon coupling with svivons around \mathbf{k}_0 (see Fig. 2), and with QE's at BZ areas of highest density of states (DOS) close to E_F , which are found in most of the cuprates around the ‘‘antinodal’’ points $(\frac{\pi}{a}, 0)$ and $(0, \frac{\pi}{a})$. If (from its four possibilities) \mathbf{k}_0 were chosen at $(\frac{\pi}{2a}, \frac{\pi}{2a})$, then the BZ areas in those cuprates, which the \mathbf{k} values contributing to the stripon states mostly come from, would be [49] at about a quarter of the BZ around $\pm\mathbf{k}^p = \pm(\frac{\pi}{2a}, -\frac{\pi}{2a})$. Creation operators $p_e^{\dagger}(\pm\mathbf{k}^p)$ and $p_o^{\dagger}(\pm\mathbf{k}^p)$ of stripon states, which are an even and an odd combination of states at \mathbf{k}^p and $-\mathbf{k}^p$, were demonstrated [50] to be compatible with the striped structure shown in Fig. 1, in areas where the stripes are directed along either the a or the b direction.

D. Hopping-induced pairing

The electronic structure obtained here for the cuprates provides a hopping-energy-driven pairing mechanism.

Diagrams for such pairing, based on transitions between pair states of stripons and QE's, through the exchange of svivons, were presented in Ref. [89]. It has been demonstrated [49], within the t - t' - J model, that there is an energy gain in inter-stripe hopping of pairs of neighboring stripons through intermediary states of pairs of opposite-spin QE's (where a svivon is exchanged when one pair is switched to the other), compared to the hopping of two uncorrelated stripons, through intermediary QE-svivon states (since the intermediary svivon excitations are avoided). The contribution of orbitals beyond the t - t' - J model to the QE states results in further gain in stripon pairing energy, due to both intra-plane and inter-plane pair hopping.

This pairing scheme provides Eliasherg-type equations, of coupled stripon and QE pairing order parameters, which can be combined to give BCS-like equations (though including strong-coupling effects) for both of them in the second order [49]. To study these equations, a domino-type two-dimensional arrangement of stripe-like inhomogeneities, including crossover between stripe segments directed in the a and the b directions, was assumed [49], and found later to be consistent with STM results [27]. An overall $d_{x^2-y^2}$ -type pairing symmetry was obtained [49], under which pair correlations are maximal between opposite-spin nearest-neighbor QE sites, and vanish between same-spin next-nearest-neighbor QE sites (see Fig. 1). Sign reversal is obtained [49] for the QE order parameter through the charged stripes. Thus, the lack of long-range coherence in the details of the stripe-like inhomogeneities, especially between different CuO_2 planes, results in features different from those of a simple $d_{x^2-y^2}$ -wave pairing (especially when c -direction hopping is involved), as has been observed [90].

E. Pairing and coherence

Within the GTC [49, 50], the phase diagram of the cuprates is largely the consequence of interplay between pairing and coherence within the regime of a Mott transition. The pairing mechanism, which depends on the stripe-like inhomogeneities, is stronger when the AF/stripes effects are stronger, thus closer to the insulating side of the Mott transition regime. Consequently, the temperature T_{pair} , below which pairing occurs, decreases with the doping level x , as is sketched in the pairing line in Fig. 3. On the other hand, phase coherence, be it of single electrons or of pairs, requires the energetic advantage of itineracy around E_F , which is easier to achieve closer to the metallic side of the Mott transition regime. Thus the temperature T_{coh} , below which coherence occurs, increases with x , as is sketched in the coherence line in Fig. 3. Thus $T_c \leq \min(T_{\text{pair}}, T_{\text{coh}})$.

For $x \gtrsim 0.19$, one has $T_{\text{pair}} < T_{\text{coh}}$, and T_c is determined by T_{pair} . Single-electron coherence, which means the existence of an FL state, then exists for $T_c < T < T_{\text{coh}}$ (see Fig. 3), as indicated by ARPES results [49, 50].

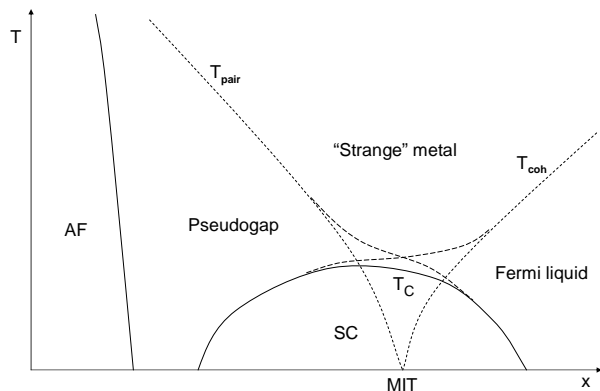


FIG. 3: A schematic phase diagram for the cuprates. The T_c line is determined by the pairing line (T_{pair}), decreasing with x , and the coherence line (T_{coh}), increasing with x . Broken lines should not be regarded as sharp lines (except when $T \rightarrow 0$), but as crossover regimes. The MIT point is a QCP where a metal-insulator transition occurs at $T = 0$ when SC is suppressed.

Within the non-FL approach used here, the stripe-like inhomogeneities are treated adiabatically; but the absence of a pairing gap results in a large svivon linewidth around \mathbf{k}_0 , and thus fast stripes dynamics, which is consistent with the existence of an FL state below T_{coh} .

For $x \lesssim 0.19$, one has $T_{\text{coh}} < T_{\text{pair}}$, and the normal-state PG, observed in the cuprates in this regime, is [49, 50] (at least partly) a pair-breaking gap at $T_c < T < T_{\text{pair}}$ (see Fig. 3). In this regime T_{pair} is generally referred to as T^* , and T_c is determined by T_{coh} . Its value is of the order of the phase stiffness, estimated through the treatment of “classical” phase fluctuations by the “X-Y” model [7]. It is given in this regime by:

$$k_B T_c \simeq k_B T_{\text{coh}} \sim \left(\frac{\hbar}{e}\right)^2 \frac{a \rho_s}{16\pi}, \quad (3)$$

$$\rho_s = \frac{4\pi e^2 n_s^*}{m_s^*} = \left(\frac{c}{\lambda}\right)^2, \quad (4)$$

in agreement with Uemura’s law [82] (based on the determination of the penetration-depth λ from μSR results).

In order to clarify somewhat the phase stiffness energy in Eq. (3), let us write it as: $N_s (\hbar K_1)^2 / 2m_s^*$, where $N_s = n_s^* (Na)^2 a / 8\pi^2$ is the average number of pairs in the volume of a slice of thickness $a / 8\pi^2$ around a plane parallel to the CuO_2 planes (assumed to be squares of length Na), m_s^* is a pair’s mass, and $K_1 = 2\pi / Na$ is the closest wave-vector point (within a plane) to the pairs’ $\mathbf{K} = 0$ ground-state point. Thus the phase stiffness is related to the energy needed (due to lattice discreteness) to excite a macroscopic number of pairs from the single-pair ground state to the first excited state. Thus, in the PG state, single-pair states are occupied (though *not* macroscopically) up to energies $\sim k_B T > k_B T_{\text{coh}}$ (which are a considerable fraction of the pairs bandwidth). Consequently moderate interactions, mixing between \mathbf{K} pair states (such as induced by phonons), are likely to mix

them, resulting in bipolaron-like localized pair states.

The application of a compressive strain, in this regime, results in the increase of $a\rho_s$, and thus also of T_{coh} and T_c [see Eq. (3)]. And indeed, ARPES results in LSCO thin films [91] show that T_c rises under such a strain. As was discussed above, the increase in T_{coh} is consistent with a move towards the metallic side of the Mott transition regime, which is reflected in the increase of the width of the bands around E_F under this strain [91].

When a junction is made, including slices of a cuprate in the SC state and in the PG state, an injection of pairs is expected to occur between them, as in p-n junctions in semiconductors. Consequently, the density of pairs in a range within the PG side of the junction could exceed the phase-stiffness limit of Eq. (3) for the occurrence of SC there. This explains the observation of a GPE in trilayer junctions of cuprate thin films [53], oriented both in the ab plane, and in the c direction. Unlike the regular proximity effect, where the range is determined by the coherence length, the range of the GPE is determined by the range where injection of carriers between the SC and PG slices occurs. This range is not related to the coherence length, and could be larger by more than an order of magnitude from it, as is observed [53].

F. Gap equations and heterogeneity

In order to understand the natures of the SC and PG states, let us regard the QE and stripon (Bogoliubov) energy bands obtained through their BCS-like equations [50]:

$$E_{\pm}^q(\mathbf{k}) = \pm \sqrt{\epsilon^q(\mathbf{k})^2 + \Delta^q(\mathbf{k})^2}, \quad (5)$$

$$E_{\pm}^p(\mathbf{k}) = \pm \sqrt{\epsilon^p(\mathbf{k})^2 + \Delta^p(\mathbf{k})^2}. \quad (6)$$

$2\Delta^q$ and $2\Delta^p$ are related to the observed pairing gap [50], as will be discussed below. They scale with T_{pair} , approximately according to the BCS factors, with an increase due to the effect of strong coupling. A d -wave pairing factor [33] is relevant for Δ^q , which has its maximum Δ_{max}^q at the antinodal points. Since the stripons reside in about a quarter of the BZ around $\pm \mathbf{k}^p$, $|\Delta^p|$ does not vary much from its mean value $\bar{\Delta}^p$, and an s -wave pairing factor is relevant for it. Thus, at low T :

$$2\Delta_{\text{max}}^q \gtrsim 4.3 k_B T_{\text{pair}}, \quad 2\bar{\Delta}^p \gtrsim 3.5 k_B T_{\text{pair}}. \quad (7)$$

The stripon bandwidth ω^p has been estimated from TEP results [48] (see below) to be ~ 0.02 eV, and by the measured T_{pair} (see Fig. 3) and the above expression, it is considerably smaller than $\bar{\Delta}^p$ in the UD regime, and exceeds its value only in the heavily OD regime. Consequently, in the UD regime, $E_{\pm}^p(\mathbf{k}) \simeq \pm |\Delta^p(\mathbf{k})|$, and the Bogoliubov transformation dictates [50] an approximate half filling of the band of the paired stripons. Thus, if all the stripons were paired, the stripon band would have been approximately half filled (thus $n^p = \frac{1}{2}$) at low T .

This is inconsistent with TEP results [48] (see below) according to which $n^p > \frac{1}{2}$ in the UD regime, and becomes $\frac{1}{2}$ for $x \simeq 0.19$.

Consequently [50], only a part of the stripions could be paired in the UD regime, while complete QE pairing (except for the nodal and localized states discussed below) is expected for $T \rightarrow 0$. Thus the PG state consists of *both* paired and unpaired stripions. Since an SC ground state is normally characterized by complete pairing for $T \rightarrow 0$, an *intrinsically* heterogenous SC state is obtained there [50], with nanoscale perfectly SC regions, where, locally, $n^p \simeq \frac{1}{2}$, and partial-pairing PG-like regions, where $n^p > \frac{1}{2}$ locally, but SC still occurs in proximity to the $n^p \simeq \frac{1}{2}$ regions. This effect is expected to be weaker, or absent, in the OD regime, where Δ^p becomes comparable, and even smaller than ω^p .

Such a nanoscale heterogeneity, was indeed observed in STM data in the SC phase [28], and it is also supported by optical results [92]. Its features are consistent with the above prediction [50] about the existence of perfectly SC regions, and (especially in the UD regime) partial-pairing PG-like regions. The size of these regions is comparable to the SC coherence length, so that SC is maintained also in the partially-paired regions.

G. Quantum critical point

The degeneracy of the paired states in a perfectly SC state is maintained by the dynamics of the stripe-like inhomogeneities [50]. Thus the free-energy gain in this state keeps them dynamical to $T \rightarrow 0$. This is not the case in the PG state (and also within PG-like regions in an heterogenous SC state), where these inhomogeneities partially freeze at low T into a glassy checkerboard structure [27, 28]. Within this structure one can observe [27] *a*- and *b*-directed stripe segments, and also $(4a) \times (4a)$ patterns obtained due to switching between *a*- and *b*-directed segments, when fluctuations occur between domino-type two-dimensional arrangements of the inhomogeneities [49].

The formation of this glassy structure is of a similar nature to CDW/SDW transitions, and orbital effects of the type of the DDW [9, 10] may also play a role. Energy is gained by creating partial or complete minigaps for the unpaired carriers (which may result in an additional superstructure [27]); but even if there is no real gap within the whole BZ, the unpaired carriers would become Anderson-localized due to their low DOS in the low- T disordered glassy structure. And indeed, low- T upturns are observed in the electrical resistivity in the PG states, either for low x , or if the SC state is suppressed, for $x \lesssim 0.19$, by applying a magnetic field [51], or by doping [52]. When such a suppression occurs, the pairing and coherence lines (see Fig. 3) meet at $T = 0$ around $x \simeq 0.19$, where an MIT occurs [50] between the FL metallic phase, and the PG non-metallic phase.

The $T = 0$ MIT point in Fig. 3 satisfies the conditions

of a QCP [81]. The stoichiometry x where it occurs is close to $x_c \simeq 0.19$, where the fractional stripion occupancy, as was determined from the TEP results [48] (see below), is $n^p = \frac{1}{2}$. The existence of the MIT close to this stoichiometry is plausible [50], because for higher doping levels the bare stripions become too packed within the charged stripes (see Fig. 1), and inter-atomic Coulomb repulsion between them is likely to destabilize the stripe-like inhomogeneities in the PG state (though the energy gain in the SC state helps maintaining them for higher x) and stabilize the homogeneous FL state.

III. PREVIOUS APPLICATIONS OF THE GTC

A. Electron spectrum

Spectroscopic measurements (as in tunneling and ARPES) based on the transfer of electrons into, or out of, the crystal, are determined by the electron's spectral function A_e , obtained by projecting the auxiliary spectral functions A^q , A^p , and A^ζ to the physical space. Such an expression was derived for A_e [49], and it includes a QE (A^q) term, and a convoluted stripion-svicon ($A^p A^\zeta$) term. From the quasi-continuum of QE bands, only few bands, which are closely related to those of physical electrons, contribute "coherent" bands, while the other QE bands contribute an "incoherent" background to A_e . Both the bands and the background include hybridized A^q and $A^p A^\zeta$ contributions, having widths including [49] an MFL-type term $\propto \omega$, and a constant term, in agreement with experiment. A_e is spanned between the upper and lower Hubbard bands, and the vicinity of E_F , and its weight around E_F is increasing with x .

Since the stripion states reside (in most cuprates) mainly in a quarter of the BZ around points $\pm \mathbf{k}^p$ [49, 50] (see above), a significant $A^p A^\zeta$ contribution to A_e close to E_F (at energies around $\bar{\epsilon}^p \pm \bar{\epsilon}^\zeta$) is obtained, with svivons around their energy minimum at \mathbf{k}_0 , in BZ areas around the antinodal points. Thus the $A^p A^\zeta$ contribution to A_e is *not* significant close to "nodal" FS crossing points, in the vicinity of $\pm(\frac{\pi}{2a}, \pm\frac{\pi}{2a})$, where A_e is determined primarily by A^q .

Thus the shape of the electron bands around the nodal points is similar to that of $\bar{\epsilon}^q$, and the (almost) T -independent "nodal kink" observed by ARPES [93, 94], closely *below* E_F , in p-type cuprates, corresponds [50] to the T -independent kink-like behavior obtained for $\bar{\epsilon}^q$ there (see above). The absence of such a kink in ARPES measurements in the n-type cuprate NCCO [95] is also consistent with the GTC, which predicts it to occur there closely *above* E_F [50] (and thus out of the range of ARPES).

On the other hand, the T -dependent "antinodal kink", observed by ARPES around the antinodal points [21, 96, 97], where its major part appears only below T_c , is due to the $A^p A^\zeta$ contribution to the electron bands there [50]. Since (see below) the opening of a pairing gap causes a

decrease in the svivon linewidth around the energy minimum at \mathbf{k}_0 (see Fig. 2), this contribution narrows down as T is decreased below T_{pair} , and especially below T_c [50], as is observed in this kink [21, 96, 97].

B. Pair-breaking excitations

Thus the antinodal kink is a spectroscopic signature of the pairing gap. Since (in a pairing state) the bandwidth of the Bogoliubov bands E_+^p and E_-^p , in Eq. (6), is small, the convoluted stripon–svivon states of energies $E_+^p \pm \bar{\epsilon}^\zeta$ and $E_-^p \pm \bar{\epsilon}^\zeta$ form [50] (for svivons around \mathbf{k}_0) spectral peaks, centered at E_+^p and E_-^p , around the antinodal points. The size of the SC gap is experimentally determined by the spacing between the closest spectral maxima on its two sides. Thus it is given by:

$$\begin{aligned} 2|\Delta^{\text{SC}}(\mathbf{k})| &= 2 \min [|\Delta^q(\mathbf{k})|, E_{\text{peak}}(\mathbf{k})], \\ E_{\text{peak}}(\mathbf{k}) &= |E_{\pm}^p(\mathbf{k} \pm \mathbf{k}_0)|. \end{aligned} \quad (8)$$

By Eq. (7), $\Delta_{\text{max}}^q > \bar{\Delta}^p$; consequently Δ^{SC} is determined by Δ^q around its zeroes at the nodal points, and by Δ^p around its maxima at the antinodal points [where $E_{\text{peak}}(\mathbf{k})$ exist]. Actually, since this convoluted stripon–svivon peak lies on the slope of the QE gap, its maximum is shifted to an energy slightly above $E_{\text{peak}}(\mathbf{k})$.

Since the QE and convoluted stripon–svivon states hybridize with each other, the states at energies $E_{\pm}^q(\mathbf{k})$, around the antinodal points, are scattered to stripon–svivon states at energies $E_{\pm}^p \pm \bar{\epsilon}^\zeta$ of magnitudes above $E_{\text{peak}}(\mathbf{k})$ (see Fig. 2 and the discussion following it). This results in the widening of the QE coherence peak [due to Eq. (5)], at the QE gap edge, to a hump [50].

In the PG state [50], the pairs lack phase coherence, and thus Eq. (5) does not yield a coherence peak in the QE gap edge. Furthermore, in this state unpaired convoluted stripon–svivon states exist [50] (see discussion above) within the gap, resulting in the widening of the low-energy svivon states, and thus of $\pm E_{\text{peak}}(\mathbf{k})$, due to scattering. Consequently, the gap-edge stripon–svivon peak is smeared, and at temperatures well above T_c the PG becomes a depression of width: $2|\Delta^{\text{PG}}(\mathbf{k})| = 2|\Delta^q(\mathbf{k})|$ in the DOS [50], in agreement with tunneling results [98, 99].

Thus the pair-breaking excitations in the SC state are characterized by [50] a peak-dip-hump structure (on both sides of the gap) in agreement with tunneling [98, 99] and ARPES results [96, 100–103]. The peak is largely contributed by the convoluted stripon–svivon states around $E_{\text{peak}}(\mathbf{k})$, the dip results from the sharp descent at the upper side of this peak, and the hump above them is of the QE gap edge and other states, widened due to the scattering to stripon–svivon states above the peak, discussed above. By Eqs. (7), and (8), Δ^{SC} and Δ^{PG} scale with T_{pair} , and thus decrease with x , following the pairing line in Fig. 3, as has been observed [50].

The heterogeneous existence, in an SC state, of perfectly SC and PG-like partial-pairing regions, discussed

above, has been observed by STM [28] through the distribution in the heights and widths of the gap-edge peak (widened due to scattering of svivons to unpaired stripions and QE’s). These STM results also show [28] that, unlike the gap-edge peak, the low energy excitations near the SC gap minimum are not affected by this heterogeneity. This is consistent with the prediction [50] [see Eq. (8)] that the SC gap is determined, around its zeroes at the nodal points, by the QE gap Δ^q . The magnitudes of the QE energies $E_{\pm}^q(\mathbf{k})$ around the nodal points, are *below* the range of E_{peak} , and convoluted stripon–svivon states, which may hybridize with them, correspond to svivons which are *not* at the vicinity of \mathbf{k}_0 , and to energies $E_{\pm}^p \pm \bar{\epsilon}^\zeta$ of magnitudes *above* E_{peak} . Thus the hybridization between them is insignificant (see Fig. 2 and the discussion following it), and the linewidths of the QE states around the nodal points are small in the SC state, and do *not* vary between the perfectly SC and PG-like regions, as the gap-edge states do.

C. Localization gaps, and nodal FS arcs

As was mentioned above, the formation of the glassy (checkerboard) structure in the PG state, and the PG-like SC regions, is self-consistently intertwined with the formation of (at least partial) minigaps and the localization of the unpaired stripions. Such gaps are formed there also in QE states around the antinodal points, which are strongly hybridized with these unpaired stripon states (convoluted with svivons around \mathbf{k}_0), and they become localized too. QE states are extended over a larger range in space than the size of the SC regions, and those with the above localization gaps can participate in the pairing process only if these gaps are (approximately) smaller than their pairing gaps.

Since the QE bandwidth is much larger than $|\Delta^q|$ [see Eq. (5)], they become almost completely paired at low T (also in the PG state), except for the QE states which have too big localization gaps to participate in the pairing process, and those at the vicinity of the nodal points. The minimal doping level $x_0 \simeq 0.05$ [67], for which SC pairing occurs, is determined by the condition that for $x \rightarrow x_0$ the number of QE states, which have sufficiently small localization gaps to be coupled to stripon states in the pairing process [49], drops below the minimum necessary for the pairing to occur.

Consequently, ARPES measurements in the SC as well as the PG state [104, 105], show that parts of FS around the antinodal points disappear, due to the formation of the QE gap (including parts which are due to localization, and parts which are due to pairing). On the other hand, arcs of the FS remain around the zero- Δ^q nodal points, where unpaired QE states persist at low T , and become localized for $T \rightarrow 0$. Such arcs continue to exist also for $x < x_0$ [106]. The $x < x_0$ regime is characterized by “diagonal stripes”, where the stripon states do not contribute at E_F [106], and transport is due to the QE’s

on the nodal arcs (with the rest of the FS missing). The modulation caused by the diagonal stripes, in a direction perpendicular to them, could be the reason for the mini-gap observed [107] by ARPES in the nodal direction in this regime.

Resistivity (ρ) measurements through $x = x_0$ [108] confirm the low- T localization on the nodal FS arcs (whether it is Anderson localization, or due to a mini-gap), and show a monotonous variation of $\rho(T)$ with x , which is not affected (except for the occurrence of SC) by the change in the striped structure or the AF transition. This indicates that the QE's on the nodal FS arcs are hardly affected by the change in the striped structure. Their hopping is likely to be dominated by t' processes [49], which do not disturb the AF order. One could distinguish between the heavily UD regime [67] of $x < x'_0 \simeq 0.09 (> x_0)$, where low T transport is largely due to QE's on the nodal FS arcs, and the rest of the cuprates phase diagram (for $x > x'_0$), where their role in transport is less important.

D. Spin excitations and the resonance mode

Tunneling results [109] show a correlation between the width of the SC gap-edge peak and the neutron-scattering resonance-mode energy [110] E_{res} . Such spin excitations are determined by the imaginary part of the spin susceptibility $\chi''(\mathbf{k}, \omega)$, and an expression for the contribution of the large- U orbitals to it has been derived in Ref. [49]. It turns out that large contributions to it are obtained from double-svicon excitations, when both svicon states are close to \mathbf{k}_0 , and their energies, ω_1 and ω_2 , either have the same sign, and contribute to $\chi''(\mathbf{k}, \omega)$ at $\omega = \pm(\omega_1 + \omega_2)$, or they have opposite signs, and contribute to it at $\omega = \pm(\omega_1 - \omega_2)$. This results (see Fig. 2) in two branches of spin excitations, a low- ω branch, having a maximum $-2\bar{\epsilon}^\zeta(\mathbf{k}_0)$ at $\mathbf{k} = \mathbf{Q} = 2\mathbf{k}_0$ (identified as the resonance mode [110, 111]), and a high- ω wide branch with an extensive minimum, spreading over the first branch [49, 50]. These branches, and also their linewidths, below and above T_c , correspond to neutron-scattering results [111–114]. [A more quantitative calculation of $\chi''(\mathbf{k}, \omega)$ is in preparation].

The width of the spin excitations is determined [50] by the scattering between QE, stripon, and svicon states, which is strong when $E^q \simeq E^p \pm \bar{\epsilon}^\zeta$, for svicon states close to \mathbf{k}_0 [where the $\cosh(\xi_{\mathbf{k}})$ and $\sinh(\xi_{\mathbf{k}})$ factors are large – see Eqs. (1) and (2) and the discussion following Fig. 2]. The existence of a pairing gap limits (especially below T_c) the scattering of the svicon states around \mathbf{k}_0 , resulting in a decrease in their linewidth. Let \mathbf{k}_{min} be the points of small svicon linewidth, for which $\bar{\epsilon}^\zeta(\mathbf{k}_{\text{min}})$ is the closest to the energy minimum $\bar{\epsilon}^\zeta(\mathbf{k}_0)$ (see Fig. 2). Often one has $\mathbf{k}_{\text{min}} = \mathbf{k}_0$, but there are cases, like that of LSCO [50], where the linewidth of $\bar{\epsilon}^\zeta$ is small not at \mathbf{k}_0 , but at close points $\mathbf{k}_{\text{min}} = \mathbf{k}_0 \pm \mathbf{q}$. The resonance mode energy E_{res} is taken here as $-2\bar{\epsilon}^\zeta(\mathbf{k}_{\text{min}})$, accounting both

for the often observed “commensurate mode” at Q , and for cases of an “incommensurate mode” [50], as observed in LSCO at $\mathbf{Q} \pm 2\mathbf{q}$ [115–117].

The determination of \mathbf{k}_{min} is [50] through the condition $E_{\text{res}} = 2|\bar{\epsilon}^\zeta(\mathbf{k}_{\text{min}})| \leq 2\tilde{\Delta}^{\text{SC}}$, where $2\tilde{\Delta}^{\text{SC}}$ is somewhat smaller than the maximal SC gap $2\Delta_{\text{max}}^{\text{SC}}$. Since $-\bar{\epsilon}^\zeta(\mathbf{k}_0)$ is zero for an AF (see Fig. 2), its value (and thus E_{res}) is expected to increase with x , distancing from an AF state. However, since its linewidth cannot remain small if $|\bar{\epsilon}^\zeta(\mathbf{k}_{\text{min}})|$ exceeds the value of $\tilde{\Delta}^{\text{SC}}$, which decreases with x , the energy E_{res} of a *sharp* resonance mode is expected [50] to cross over from an increase to a decrease with x when it approaches the value of $2\tilde{\Delta}^{\text{SC}}$, as has been observed [110]. This crossover could be followed [50] by a shift of the resonance wave vector $2\mathbf{k}_{\text{min}}$ from the AF wave vector \mathbf{Q} to incommensurate wave vectors.

E. The gap-edge peak

By the above scattering conditions [50], svicon energies $\bar{\epsilon}^\zeta$ have a small linewidth within the range $|\bar{\epsilon}^\zeta| \leq |\bar{\epsilon}^\zeta(\mathbf{k}_{\text{min}})|$. Consequently, the gap-edge peaks of the convoluted stripon–svicon states of energies $E_{\pm}^p \pm \bar{\epsilon}^\zeta$, centered at $\pm E_{\text{peak}}$ [see Eq. (8)], have a “basic” width:

$$W_{\text{peak}} = -2\bar{\epsilon}^\zeta(\mathbf{k}_{\text{min}}) = E_{\text{res}}. \quad (9)$$

Additional contributions to the width of this peak come from the svicon and stripon linewidths, and from the dispersion of $E_{\pm}^p(\mathbf{k} \pm \mathbf{k}')$ when $\bar{\epsilon}^\zeta(\mathbf{k}_{\text{min}}) \lesssim \bar{\epsilon}^\zeta(\mathbf{k}') \lesssim 0$ (see Fig. 2). This result explains [50] the observed correlation (for different doping levels) between the peak's width, and E_{res} [109].

Studies of the pair-breaking excitations in the SC state by ARPES [96, 100–103] confirm also the \mathbf{k} dependence predicted by the GTC [50]. The convoluted stripon–svicon states contribute over a range of the BZ around the antinodal points a single weakly-dispersive gap-edge peak at $E_{\text{peak}}(\mathbf{k})$. Most of the measurements were performed on bilayer BSCCO, where in addition to this peak there are around the antinodal points bilayer-split QE bands, the bonding band (BB) and the antibonding band (AB), contributing two humps around the gap [96, 100, 101]. The AB lies very close to E_{F} on the SC gap edge through the antinodal BZ range, and it almost overlaps with $E_{\text{peak}}(\mathbf{k})$ in the OD regime, where they both appear as narrow peaks [96, 100].

The BB, on the other hand, disperses considerably, crossing E_{F} , and contributes a clearly distinguished hump [96, 100, 101]. In the range where the QE BB approaches $E_{\text{peak}}(\mathbf{k})$, the fact that the electron band is formed by their hybridized contributions results in the appearance of the antinodal kink [21, 96, 97] (discussed above), due to the narrowing of the peak, as T is lowered below T_c . The width of the hump states depends on the rate of their scattering to stripon–svicon states. Since the svicons are dressed by phonons, an anomalous

isotope effect is obtained for the width, and thus also for the position of the hump states [21].

The peak-dip-hump structure has been observed also in tunneling [99] and ARPES [102] measurements in single-layer BSCO and BSLCO, proving that it is not just the effect of bilayer splitting [50]. Recent ARPES measurements in OD single-layer TBCO [103] show the existence of a gap-edge peak, which could be identified with $E_{\text{peak}}(\mathbf{k})$, over a range of the BZ around the antinodal points. It disperses over a range ~ 0.02 eV, which is comparable with the SC gap, consistently with the GTC prediction [50] for the OD regime.

Low-temperature ARPES results for the spectral weight within the *sharp* SC gap-edge peak, integrated over the antinodal BZ area [118, 119], show a maximum for $x \simeq 0.19$. This is expected by the GTC [50], assuming that the integrated spectral weight is counted within the stripon–svivon peak around E_{peak} in regions where this peak is sharp. If the number of svivon \mathbf{k} states contributing to that peak (see Fig. 2) does not vary significantly with doping in the range of interest, then the measured integrated peak counts the number of hole-like pair-breaking excitations of stripions within the E_{peak}^p band [see Eq. (6)], in regions where the peak is sharp.

For the intrinsically heterogeneous $x \lesssim 0.19$ regime, discussed above, this number increases with x because of the increase in the fraction of space covered by the perfectly SC regions (where the stripon band is approximately half full and the stripon–svivon states contribute a *sharp* gap-edge peak). For the $x \gtrsim 0.19$ regime there are no PG-like regions, and the peak is sharp wherever it exists. Thus the measured integrated peak counts there the number of hole-like pair-breaking excitations of stripions within the E_{peak}^p band, which is decreasing with the increase of x below half filling of the stripon band [50]. Note that the contribution of the QE AB to the ARPES peak had to be omitted [119] in order to get the decrease of the peak weight for $x \gtrsim 0.19$, confirming the GTC prediction that this behavior is due to the stripon–svivon gap-edge peak.

F. Asymmetry of the tunneling spectrum

One of the features of the tunneling spectrum in the cuprates [28, 98] is its asymmetry with higher DOS for hole- than particle-excitations. This asymmetry is extending beyond the limit of the presented spectrum, few tenths of an eV on both sides of E_F . Within the GTC, high- T_c in the cuprates is occurring in the regime of a Mott transition, where the spectral function $A_e(\omega)$ is spanned between the upper and lower Hubbard bands and the vicinity of E_F . As was discussed above [49], $A_e(\omega)$ has a large incoherent part, and its magnitude is decreasing when ω is varied from the Hubbard bands to the energy space between them.

In p-type cuprates E_F is closer to the (Zhang-Rice-type) lower Hubbard band, and thus $A_e(\omega)$ is descending when ω is varied from below E_F to above it (Anderson

and Ong [120] demonstrated such a behavior within the t - J model), in agreement with the observed asymmetry in the tunneling spectrum [28, 98]. In n-type cuprates, E_F is closer to the upper Hubbard band, and thus an *opposite* asymmetry is expected in the tunneling spectrum there (with higher DOS for particle- than hole-excitations), in agreement with results in n-type NCCO [121] and “infinite-layer” SLCO [122].

G. Transport properties

1. Expressions within the one-band approximation

The normal-state transport properties have been a major mystery in the cuprates. The author has been involved from the start in attempts to understand the anomalous TEP, resistivity, and Hall constant [123, 124]. Their correct treatment, within the GTC, though not including the effects of the PG, was first presented in Ref. [48]. Even though, the dynamics of the stripe-like inhomogeneities is fast above T_{pair} , their adiabatic treatment is still expected to be a reasonable approximation for the evaluation of the transport properties. Their derivation, within the ab plane, is based on linear-response theory. A condition used is that the direct current (DC) \mathbf{j} could be expressed as a sum of QE (\mathbf{j}^q) and stripon (\mathbf{j}^p) terms which are proportional to each other with an approximately T -independent proportionality factor α . Thus:

$$\mathbf{j} = \mathbf{j}^q + \mathbf{j}^p \cong \frac{\mathbf{j}^q}{1 - \alpha} \cong \frac{\mathbf{j}^p}{\alpha}. \quad (10)$$

As is discussed further below, in relation to optical conductivity, this condition is a consequence of the assumption that the contribution of the CuO_2 planes to transport is derived, dominantly, from *one* electron band of the homogeneous planes. The formation of stripe-like inhomogeneities results in separate contributions of QE’s and stripions, but the stripes dynamics results in DC based on the band of the averaged homogeneous planes. The coefficient α depends on the inhomogeneous structure, which determines how \mathbf{j} is split between \mathbf{j}^q and \mathbf{j}^p .

Transport can be treated using the separate QE and stripon chemical potentials, μ^q and μ^p (due to the large- U constraint), discussed above. When an electric field \mathbf{E} is applied, Eq. (10) is satisfied by the formation of gradients $\nabla\mu^q$ and $\nabla\mu^p$ [48], where the homogeneity of charge neutrality imposes:

$$\frac{\partial n_e^q}{\partial \mu^q} \nabla\mu^q + \frac{\partial n_e^p}{\partial \mu^p} \nabla\mu^p = 0. \quad (11)$$

Here n_e^q and n_e^p are the contributions of QE and stripon states to the electrons occupation. Because of the small stripon bandwidth, it is convenient to introduce [48]:

$$N_e^q \equiv \frac{\partial n_e^q}{\partial \mu^q}, \quad M_e^p(T) \equiv T \frac{\partial n_e^p}{\partial \mu^p}, \quad (12)$$

where N_e^q is almost temperature independent, and $M_e^p(T)$ saturates at temperatures above the stripon bandwidth to a constant $n^p(1 - n^p)$ [48].

The chemical potential gradients introduce “chemical fields”, resulting in different effective fields for QE’s and stripons [48]:

$$\boldsymbol{\mathcal{E}}^q = \mathbf{E} + \nabla\mu^q/e, \quad \boldsymbol{\mathcal{E}}^p = \mathbf{E} + \nabla\mu^p/e, \quad (13)$$

and by Eqs. (11), (12), and (13), one gets:

$$\mathbf{E} = \frac{M_e^p(T)\boldsymbol{\mathcal{E}}^p + N_e^q T \boldsymbol{\mathcal{E}}^q}{M_e^p(T) + N_e^q T}. \quad (14)$$

Effective QE and stripon conductivities σ^q and σ^p are introduced through the expressions:

$$\boldsymbol{\mathcal{E}}^q = \mathbf{j}/\sigma^q(T), \quad \boldsymbol{\mathcal{E}}^p = \mathbf{j}/\sigma^p(T), \quad (15)$$

and related expressions are used [48] to introduce effective QE and stripon Hall numbers n_H^q and n_H^p , and TEP’s S^q and S^p . Using Eq. (14), the following expressions are then obtained [48] for the electrical conductivity (σ), Hall number (n_H), and TEP (S):

$$\sigma = \frac{M_e^p(T) + N_e^q T}{M_e^p(T)/\sigma^p(T) + N_e^q T/\sigma^q(T)}, \quad (16)$$

$$n_H = \frac{M_e^p(T) + N_e^q T}{M_e^p(T)/n_H^p + N_e^q T/n_H^q}, \quad (17)$$

$$S = \frac{M_e^p(T)S^p(T) + N_e^q T S^q(T)}{M_e^p(T) + N_e^q T}. \quad (18)$$

At low T , for $x \gg x'_0$, the value of $M_e^p(T)$ is generally about an order of magnitude greater than $N_e^q T$. Consequently, by Eqs. (11) and (12), $\nabla\mu^p \cong 0$ and $\nabla\mu^q \cong -e\mathbf{E}$. Thus, by Eq. (13), $\boldsymbol{\mathcal{E}}^p \cong \mathbf{E}$, $\boldsymbol{\mathcal{E}}^q \cong 0$, and by Eqs. (16), (17) and (18), the transport coefficients are dominantly stripon-like at low T , both above and below T_c , and a crossover to a QE-like behavior is occurring when T is increased through the stability temperature regime. When pairing gaps exist, μ^q and μ^p are within these gaps, and their existence results in some decrease in the low- T value of $M_e^p(T)$ in Eq. (12), resulting in some increase in the QE contribution to transport at low T . The assumption that $M_e^p(T) \gg N_e^q T$, at low T , breaks down when x approaches x'_0 (towards the heavily UD regime), where the PG and SC gap are large. As was discussed above, low- T transport for $x < x'_0$ is largely due to QE’s, which are on the nodal FS arcs, for the unpaired carriers [67].

2. Transport results

The above expressions were applied [48], using a minimal set of realistic parameters. The transport coefficients were calculated as a function of T , for five stoichiometries of p-type cuprates, ranging from $n^p = 0.8$, corresponding to the UD regime, to $n^p = 0.4$, corresponding to the

OD regime. GTC auxiliary spectral functions, and zero-energy T -dependent scattering rates were used, and also impurity-scattering T -independent terms. The stripon band was modeled by a “rectangular” spectral function A^p of width ω^p , for which was a value of ~ 0.02 eV was found to be consistent with experiment.

The TEP results depend strongly on n^p , and reproduce very well [48] the doping-dependent experimental behavior [123, 125], which has been used to determine stoichiometry. The low- T stripon-like result saturates at $T \gtrsim 200$ K to a constant $(k_B/e) \ln[n^p/(1 - n^p)]$ [48]. But then a crossover starts towards a QE-like linear behavior, for which a negative slope is predicted [48], in agreement with experiment [125]. The stripon term $S^p(T)$ vanishes for $n^p = \frac{1}{2}$, and then the TEP is determined by negative-slope QE term $S^q(T)$, corresponding experimentally to $x = x_c \simeq 0.19$. Also the results for the Hall coefficients [48] reproduce very well the experimental behavior [126, 127]. The approximately linear increase of n_H with T is due to its crossover from a low- T stripon-like n_H^p towards a QE-like n_H^q . The signs of n_H^p and n_H^q are the same, both determined by the nature of the one-band current \mathbf{j} of the averaged homogeneous planes. Thus n_H is *not* expected to change sign with T within the assumed one-band approximation [leading to Eq. (10)].

The calculated T dependence of ρ [48] is linear at high T , flattening to (stripon-like) “superlinearity” at low T (for all stoichiometries). Experimentally [85], the low- T behavior crosses over from “sublinearity” in the UD regime (and a non-metallic upturn at lower T if T_c is low enough), to superlinearity in the OD regime. As is discussed below, in relation to optical conductivity, the sublinear behavior is the effect of reduced scattering rate in the PG state. The low- T upturn results from the localization in this state, discussed above. The crossover to superlinear behavior (predicted here) in the OD regime is a natural consequence of the disappearance of the PG with increasing x (see Fig. 3). The linear T -dependence of ρ persists to low- T for $x \sim 0.19$ [128], which is due to quantum criticality [81] close to the QCP (discussed above). In the critical region there is only one energy scale, which is the temperature, resulting in MFL-type behavior [5].

The TEP in n-type cuprates is normally expected [48] to behave similarly to the TEP in p-type cuprates, but with an opposite sign and slope. Results for NCCO [129] show such behavior for low doping levels, but in SC doping levels the high- T slope of S is changing from positive to negative, and its behavior resembles that of OD p-type cuprates. This led [48] to the suggestion that NCCO may be not a real n-type cuprate, its stripions being based on holon states (as in p-type cuprates).

More recent results on the n-type infinite-layer SLCO [130] do show TEP results for an SC cuprate which have the opposite sign and slope than those calculated for p-type cuprates [48], as is expected for real n-type cuprates (thus with stripions based on excitation states). It is likely that the sign of the TEP slope in NCCO changes with

doping because the one-band approximation, leading to Eq. (10), becomes invalid. This is indicated by ARPES [131], and by the change with temperature of the sign of the Hall constant of NCCO [129], at the stoichiometries where the sign of the slope of the TEP has changed (see above). Also, in YBCO, the contribution of an additional band of the chains' carriers results in an almost zero high- T slope of the TEP [123], rather than the negative slope predicted by the GTC [48].

H. Superfluid density

The Uemura's plots [82] give information about the effective density of SC pairs n_s^* through Eq. (4). One of the mysteries of the cuprates has been the boomerang-type behavior [69] of these plots for $x \gtrsim 0.19$. The author connected this behavior, as early 1994 [88], with the fact that the (presently called) stripon band passes through half filling. As was mentioned above, the effect of pairing is the hybridization between stripon and QE pairs [49]. The determination of λ in the μ SR measurements [82] is through DC in a magnetic field, and as was determined in Eqs. (16)–(18), and the discussion following them, DC below T_c is stripon like for lightly UD, optimal (OPT), and OD stoichiometries.

Thus n_s^* determined from λ , through μ SR measurements [82], approximately corresponds, in this regime, to the density of stripon pairs. As was mentioned above, the stripon band is half full for $x = x_c \simeq 0.19$, and consequently n_s^* is maximal around this stoichiometry, being determined (for p-type cuprates) by the density of hole-like stripon pairs for $x < x_c$, and of particle-like stripon pairs for $x > x_c$. This result is not changed by the intrinsic heterogeneity [50] for $x \lesssim 0.19$, discussed above; T_c is determined there, through Eq. (3), by the average value of n_s^* , determined by measuring the penetration depth which [68] is larger than the sizes of the heterogenous regions [28].

In the crossover to the heavily UD ($x < x'_0$) regime, the behavior of low- T DC crosses over, as was discussed above, from being stripon-like to being QE-like. Thus, the effective superfluid density $n_{s,\text{eff}}$ (derived from the measured λ) becomes dominated, for $x < x'_0$, by the QE contribution to the superfluid. As was discussed above, the glassy structure in PG-like SC regions results in the formation of localization gaps for QE states around the antinodal points, thus preventing their contribution to the superfluid when their localization gaps are, approximately, greater than their pairing gaps. Since the fraction of the QE states with localization gaps, which are small enough to contribute to the superfluid, decreases as $x \rightarrow x_0$ (and $n_s^* \rightarrow 0$), the contribution of QE's to the superfluid decreases then *faster* than its density n_s^* . Thus, it is reasonable to assume in this regime an approximate expression of the form $n_{s,\text{eff}} \propto (n_s^*)^\beta$, where $\beta > 1$. Consequently, Eqs. (3) and (4) yield in this regime $T_c \propto n_s^* \propto n_{s,\text{eff}}^{1/\beta}$. And indeed, penetration-depth mea-

surements in the heavily UD regime [86] reveal such a behavior with $\beta = 2.3 \pm 0.4$.

IV. OPTICAL CONDUCTIVITY WITHIN THE ab PLANE

A. One-band formalism

It is assumed that the optical conductivity, within the ab plane, is dominantly contributed (within the frequency range of interest) by one band [17] of the homogeneous planes. Thus the relevant Hamiltonian is expressed as:

$$\mathcal{H} = \sum_{\mathbf{k},\sigma} \epsilon_b(\mathbf{k}) d_\sigma^\dagger(\mathbf{k}) d_\sigma(\mathbf{k}) + \mathcal{H}_{\text{int}}. \quad (19)$$

It includes a “bare band” [$\epsilon_b(\mathbf{k})$] one-particle term, and a two-particle interaction term \mathcal{H}_{int} . \mathcal{H} determines electron velocities $\mathbf{v}(\mathbf{k})$, in terms of which the electrical current operator (due to it) is expressed as:

$$\hat{\mathbf{j}} \cong -e \sum_{\mathbf{k},\sigma} \mathbf{v}(\mathbf{k}) d_\sigma^\dagger(\mathbf{k}) d_\sigma(\mathbf{k}). \quad (20)$$

The electron creation and annihilation operators $d_\sigma^\dagger(\mathbf{k})$, and $d_\sigma(\mathbf{k})$, are expressed in terms of the auxiliary-space QE and convoluted stripon–svivon operators. Consequently the ω -dependent electrical current, in the presence of an electric field $\mathbf{E}(\omega)$, can be expressed as a sum of a QE (\mathbf{j}^q), a stripon–svivon (\mathbf{j}^p), and a mixed (\mathbf{j}^{qp}) term:

$$\mathbf{j}(\omega) = \langle \hat{\mathbf{j}}(\omega) \rangle = \mathbf{j}^q(\omega) + \mathbf{j}^p(\omega) + \mathbf{j}^{qp}(\omega). \quad (21)$$

Since the svivons carry no charge, their effect on \mathbf{j}^p is through field-independent spin occupation factors. On the other hand, \mathbf{j}^{qp} involves field-induced transitions between QE and stripon–svivon states, and thus svivon excitations. Since $A^\zeta(\omega = 0) = 0$, the contribution of \mathbf{j}^{qp} to Eq. (21) vanishes for $\omega \rightarrow 0$, and Eq. (10) can be used for DC.

B. The f–sum rule

If the entire frequency spectrum were considered, the real part of the electrons' contribution to the optical conductivity $\sigma(\omega) = \mathbf{j}(\omega)/\mathbf{E}(\omega)$ should obey [37, 38, 54–56] the f–sum rule $\int_0^\infty \Re\sigma(\omega) d\omega = \pi n e^2 / 2m_e$, where n and m_e are the electrons' (total) density and (unrenormalized) mass. By considering only the one-band contribution of \mathcal{H} in Eq. (19), one obtains the partial f–sum rule [37, 38, 54–56] (V is the volume):

$$\int_0^\infty \Re\sigma(\omega) d\omega = \frac{\pi e^2}{2V} \sum_{\mathbf{k},\sigma} \frac{\langle d_\sigma^\dagger(\mathbf{k}) d_\sigma(\mathbf{k}) \rangle}{m_b(\mathbf{k})}, \quad (22)$$

$$\frac{1}{m_b(\mathbf{k})} \equiv \frac{1}{\hbar^2} \frac{\partial^2 \epsilon_b(\mathbf{k})}{\partial \mathbf{k}^2}. \quad (23)$$

The effective mass $m_b(\mathbf{k})$, appearing in Eq. (22), is within the bare band in \mathcal{H} [Eq. (19)]. The effect of the \mathcal{H}_{int} term there is through the occupation factors $\langle d_\sigma^\dagger(\mathbf{k})d_\sigma(\mathbf{k}) \rangle$ in Eq. (22). Since a large- U -limit method is applied here for \mathcal{H}_{int} , an optical determination of $\langle d_\sigma^\dagger(\mathbf{k})d_\sigma(\mathbf{k}) \rangle$ requires the consideration of transitions including states in the lower, as well as the upper Hubbard band (both in p-type cuprates and in n-type cuprates), which means the inclusion of energies $\omega \gtrsim 2$ eV in the integral in Eq. (22). This conclusion is supported by the XAS results [132] for the position of the chemical potential in p- and n-type cuprates.

The optical conductivity can be determined experimentally by reflectance measurements and a Kramers–Kronig analysis [56, 66], and the integral in Eq. (22) can be carried out up to an experimental cutoff frequency ω_{co} . This procedure has to be modified in the SC state [56, 66], where the superfluid spectral weight, contributing to the integral, comes from a δ -function term in $\Re\sigma(\omega)$ [55]. This spectral weight equals $\omega_{\text{ps}}^2/8$, where ω_{ps} is the superfluid plasma frequency, and it can be determined [56, 66] by ellipsometry measurements, including the evaluation of the real part of the dielectric function $\epsilon(\omega)$, and the application of the relation: $\Re\epsilon(\omega) = \epsilon(\infty) - (\omega_{\text{ps}}/\omega)^2$.

This derivation of the superfluid plasma frequency provides an optical method to determine the value of the parameter ρ_s [see Eq. (4)], through the relation $\rho_s = \omega_{\text{ps}}^2$. There is a question concerning the relation between this optically-derived value and the value of ρ_s derived through measurements of the penetration depth λ in a magnetic field, by methods like μSR . The carrier masses, determined by the two methods, are not identical; while the optical measurements yield the bare-band mass $m_b(\mathbf{k})$, appearing in Eq. (22), carriers dynamics in a magnetic field depends on the effective mass m_s^* of the pairs. The considerable reduction of m_s^* compared to the stripon’s mass is the driving force of the GTC pairing mechanism [49].

And indeed, it turns out [68] that the *ab* plane penetration depth determined optically, is about twice the value determined by μSR . Also, as was discussed above, the stripons’ band is half full for $x \simeq 0.19$, and m_s^* changes there from being hole like to being particle like, resulting in a boomerang-type behavior of ρ_s in the OD regime (thus changing from increasing to decreasing with x), in agreement with μSR results [69]. On the other hand $m_b(\mathbf{k})$, which determines the optical ρ_s , corresponds to the bare mass of the averaged homogeneous CuO_2 planes, which is hole like, and does not pass through half filling within the SC doping range. Thus the optically determined ρ_s is expected to rise with x , and have no boomerang-type behavior, as has been observed [70].

C. “Violations” of the f -sum rule

In ordinary SC’s [55], the formation of an SC gap in $\Re\sigma(\omega)$ is followed by the transfer of spectral weight of

magnitude $\omega_{\text{ps}}^2/8$ from it to the δ -function term. Thus, the value of the integral in Eq. (22) (including the $\omega_{\text{ps}}^2/8$ contribution in the SC state) is not expected then to change between the normal and the SC state, when ω_{co} is taken sufficiently above the gap energy. Ellipsometric measurements in p-type cuprates [57–60] confirm such behaviour in the OD regime, while for UD and OPT stoichiometries, this behavior was found to be “violated” even when ω_{co} values above 2 eV were used. This “violation” points to the transfer of spectral weight below T_c from energies $\gtrsim 2$ eV to the vicinity of E_F (its validity is confirmed in a recent debate about it [133]).

There have been theoretical suggestions trying to explain this transfer of spectral weight as being due to a mechanism of pairing from a non-FL normal state, to an “FL SC” state [37], due to pairing phase fluctuations [38], or due to pairing via spin fluctuations within the nearly AF FL model [39]. But the high energy scale $\gtrsim 2$ eV involved is hard to understand unless it is assumed that the spectral weight is transferred from *both* the lower and the upper Hubbard bands [49, 50] (thus beyond the range of applicability of the t - t' - J model). As was discussed above, the spectral weight in the vicinity of E_F is increasing with x at the expense of the weight in the upper and lower Hubbard bands far from it, resulting in an increase in the itineracy of the carriers. The change in x is provided by doping atoms out of the CuO_2 planes. These atoms contribute electronic states close to E_F [and thus also contribute to $\sigma(\omega)$], from which charge is transferred to the CuO_2 planes.

The UD and OPT stoichiometries, where the transfer of spectral weight at T_c has been observed [57–60], are those where the SC transition is from the PG state (see Fig. 3). As was discussed above, the transition there is due the establishment of phase coherence of existing localized pairs, turning them into a superfluid. There are two possible mechanisms (or their combination) for an accompanying transfer of spectral weight from the Hubbard bands to the vicinity of E_F , both driven by the free energy gain in the SC state. The first one is that this transfer of spectral weight is associated with the increased itineracy of the pairs in the superfluid. The second mechanism is that since the free energy gain due to SC is determined (like T_c) by the phase stiffness, which scales [see Eqs. (3) and (4)] with the density of pairs within the CuO_2 planes, it drives further charge transfer from the doped atoms to the planes below T_c . This results in transfer of spectral weight from the Hubbard bands to the vicinity of E_F , as if x were increased. On the other hand, in the OD regime the SC transition is more BCS-like, due to pairing of electrons in an FL state, and such a transfer of spectral weight is expected less, if at all, within both of the above mechanisms.

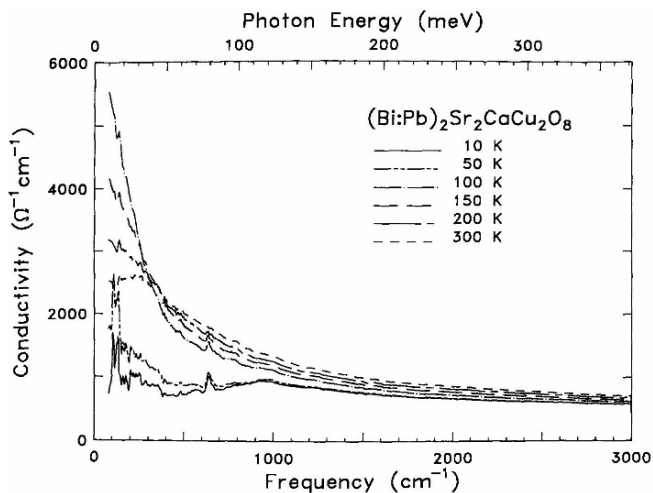


FIG. 4: Optical conductivity $\Re\sigma(\omega)$, presented by Tanner *et al.* [66], at six temperatures.

D. Optical carriers around optimal stoichiometry

1. Contributions to the effective density

An experimental study of the optical conductivity, and of the partial f-sum rule, as a function ω_{co} , for a eight different cases of p-type cuprates near OPT doping, was carried out by Tanner *et al.* [66]. A typical curve of $\Re\sigma(\omega)$, for different temperatures, is shown in Fig. 4. The electron mass m_e was chosen for $m_b(\mathbf{k})$ in Eq. (22), which is unjustified beside being a working assumption (it is not clear at this point whether an effective mass derived in an LDA-based calculation would be an appropriate choice either).

A value $\omega_{co} \simeq 12000 \text{ cm}^{-1}$ was chosen [66] in order to avoid the effect of the “charge transfer” band, and count mainly the carriers in the conduction band. As can be concluded, *e.g.*, from the measured position of the chemical potential [132], such a choice of ω_{co} in Eq. (22) does *not* count the contribution of most of the excitation-based states of the upper Hubbard band (ignored in the $t-t'-J$ model), while it does count the contribution of most of the holon-based states of the (Zhang-Rice-type) lower Hubbard band (considered in the $t-t'-J$ model). Also the contribution of states of the doped atoms (out of the CuO_2 planes) is counted if they are close enough to E_F . In YBCO this corresponds to the chains states, and they contribute considerably in measurements with polarization in the chains direction (b).

Optical carriers’ densities derived through this experimental analysis [66] are presented in Table I. One derived quantity is the effective number N_{eff}/Cu of carriers per Cu atom at $T \simeq 100 \text{ K}$ (above T_c). Most values are found to be around 0.4–0.5, except for a lower value of 0.15 for monolayer LCO, and a higher value of 0.59 (due to the contribution of the chains’ carriers) for YBCO with the

polarization taken in the b direction. It may be misleading to connect this N_{eff} with an actual number of carriers, because the contribution of the upper-Hubbard-band states is not integrated in Eq. (22). These states are essential to determine the number of carriers contributed by the QE’s, which form bands *combining* states of the lower and the upper Hubbard bands. On the other hand the number of carriers contributed by stripons could be well described just within the frame of the integrated lower-Hubbard-band states.

Two other types of carriers’ densities [66], presented in Table I, may have more physical significance. The first one is the number N_s/Cu of the superfluid carriers per Cu atom, which was determined (as was explained above) from the δ -function term in $\sigma(\omega)$ at $T \simeq 10 \text{ K}$. The second one is the number N_D/Cu of Drude carriers per Cu atom (at $T \simeq 100 \text{ K}$). It was determined by fitting $\sigma(\omega)$ to the contributions of a number of oscillators, including a Drude oscillator at zero frequency, and Lorentzian oscillators at higher frequencies. N_D was obtained by integrating over the Drude contribution, which introduces (for $T > T_c$) the major low- ω contribution to $\sigma(\omega)$ [66] in Fig. 4.

Both N_D and N_s are related to the number of carriers involved in DC conductivity, which as was shown in Eq. (16), and the discussion following it, is dominantly stripon-like at low T , for the stoichiometry studied. Thus N_D and N_s approximately correspond to the number of stripon “holes”, where N_s has somewhat larger QE contribution due to the effect of the gap on Eq. (12). The contribution to the current in Eq. (21) of $\mathbf{j}^{qp}(\omega)$ (due to transitions between QE and stripon–svivon states) could be neglected in the treatment of DC above, but it does result in much of the non-Drude (often called mid-IR) contribution to $\sigma(\omega)$ [66] in Fig. 4. The dressing by phonons, discussed above, is reflected in signatures of their structure there. Also are included in this term QE contributions which (as was discussed above) are largely “blocked” at low ω and T by the QE chemical potential gradient [see Eq. (13)], satisfying there $\nabla\mu^q \simeq -e\mathbf{E}$.

2. Striapon-like carriers

Thus, it is not surprising that the ratios N_s/N_D [66], presented in Table I, are close to one (ranging between 0.87 and 0.95, except for values around 0.80 for LCO and YBCO with polarization in the b direction). If all the Drude carriers were paired, the somewhat larger QE contribution to N_s would have yielded for it a larger value than N_D . However, since as was discussed above, there are some unpaired carriers for OPT stoichiometry, in the PG-like heterogenous regions [as can be seen in $\sigma(\omega)$ below T_c [66] in Fig. 4], one gets somewhat smaller N_s than N_D . The lower N_s/N_D ratio in YBCO is due to the contribution of the chain carriers, whose pairing could be approximately regarded as induced by proximity [8]. Since the QE contribution to the carriers’ density above

TABLE I: Effective number of carriers per copper in a variety of cuprate materials, presented by Tanner *et al.* [66], . N_{eff} is the total doping-induced carrier density, N_s the number of superfluid carriers, and N_D the number of Drude carriers. Note that the number of coppers in $\text{YBa}_2\text{Cu}_3\text{O}_7$ was taken as 2 with polarization (Pol.) along the a -axis and as 3 for polarization along the b -axis.

Material	T_c (K)	Pol.	N_{eff}/Cu	N_s/Cu	N_D/Cu	N_s/N_{eff} %	N_s/N_D %
$\text{La}_2\text{CuO}_{4+x}$	40	ab	0.15	0.028	0.035	19	80
$\text{Bi}_{1.57}\text{Pb}_{0.43}\text{Sr}_2\text{CaCu}_2\text{O}_8^{\dagger}$	79	ab	0.37	0.085	0.097	23	87
$\text{Bi}_2\text{Sr}_2\text{CaCu}_2\text{O}_8^{\ddagger}$	85	a	0.44	0.100	0.105	23	95
$\text{Bi}_2\text{Sr}_2\text{CaCu}_2\text{O}_8^{\S}$	85	b	0.48	0.090	0.096	19	94
$\text{YBa}_2\text{Cu}_3\text{O}_7^{\P}$	91	a	0.44	0.096	0.104	22	92
$\text{YBa}_2\text{Cu}_3\text{O}_7^{\ddagger}$	91	b	0.59	0.125	0.16	21	78
$\text{YBa}_2\text{Cu}_3\text{O}_5^{\S}$	92	ab	0.44	0.082	0.093	19	88
$\text{Tl}_2\text{Ba}_2\text{CaCu}_2\text{O}_8^{\ddagger}$	110	ab	0.54	0.115	0.13	21	88
Typical uncertainties	2		± 0.03	± 0.01	± 0.01	$\pm 1\%$	$\pm 4\%$

The sources of the crystals were:

^aAmes laboratory;

^bEFP de Lausanne;

^cUniversity of Wisconsin;

^dUniversity of Illinois;

^eUniversity of Texas.

T_c increases with T , the lower T_c in LCO is consistent with a lower N_s/N_D ratio in it.

As was discussed above, the TEP results [48] indicate a half-filled stripon band for $x = x_c \simeq 0.19$. Thus, for the striped structure shown in Fig. 1, the OPT stoichiometry (see Fig. 3), around which the measurements by Tanner *et al.* [66] were carried out, corresponds to a number of $N_{\text{con}}/\text{Cu} \simeq 0.125 \times 0.17/0.19 = 0.11$ stripon hole carriers per Cu atom. The values of N_s/Cu and N_D/Cu for most of the cases [66] in Table I are quite close to 0.10, except for smaller values for LCO, and larger values for YBCO with polarization in the b direction.

This overall agreement is surprisingly good, considering the fact that m_e was used for $m_b(\mathbf{k})$ in Eq. (22). The deviation in YBCO is understood due to the contribution of the chains' carriers. The deviation in LCO could be because $m_b(\mathbf{k})/m_e$ is significantly larger than one there. Pavarini *et al.* [15] have shown that when the parameters for a one-band approximation are derived from first-principles calculations, cuprates with larger maximal T_c have larger t' hopping parameters, and thus smaller $m_b(\mathbf{k})$. So having larger $m_b(\mathbf{k})/m_e$ for LCO than for the other cuprates studied (in agreement with Ref. [15]) is consistent with its considerably lower T_c . Also for TBCCO, which has higher T_c than the other cuprates studied, its somewhat larger values of N_s/Cu and N_D/Cu , than of the other cuprates presented in Table I, corresponds to its smaller $m_b(\mathbf{k})/m_e$.

3. Tanner's law and its resolution

The puzzling result of Tanner *et al.* [66] (known as Tanner's law) is that, for all the cases presented in Table I, N_s/N_{eff} ranges between 0.19 and 0.23, which means that that N_{eff} equals 4-5 times the number of stripon carriers. If the integration through Eq. (22) were extended to include the contribution of the upper-Hubbard-band states, *but* omitting the contribution of bands not included in \mathcal{H} in Eq. (19), than the number of carriers per Cu atom would have been $1 - x$ (since the bare band is short by $x/2$ from being half full for each spin state). For OPT stoichiometry this corresponds to about 0.83 carriers per Cu atom, which is greater than the (N_{eff}/Cu) values measured [66] on the basis of partial integration (omitting the upper-Hubbard-band states), and presented in Table I. It is, however, unrealistic to count *just* the contribution of the conduction-band carriers if the integration range in Eq. (22) is extended to include the upper-Hubbard-band states, since they overlap with other bands.

An analysis of $\sigma(\omega)$ on the basis of the lower-Hubbard-band states *alone* (counted in Ref. [66]) could be made, in analogy to the Kohn-Sham approach [134], by replacing \mathcal{H} in Eq. (19) by an effective Hamiltonian of small- U carriers, of the same spin symmetry as the carriers in the real system. In this system an effective time- and spin-dependent single-particle potential is introduced in order to simulate (at least approximately) the many-body effects (causing the existence of the upper-Hubbard-band) occurring in the real system. As was shown in Eq. (16), and the discussion following it, such a many-body effect is that at low ω (thus DC) and T the contribution of

QE's to transport is largely blocked around OPT stoichiometry by the QE chemical potential gradient.

In the effective system the large- U constraint, which results in different chemical potentials for QE's and stripsons, doesn't exist, and a single-particle potential has to replace it as a mechanism for blocking the contribution of QE's, but not of stripsons, to conductivity at low T and ω . This effective potential has to be dynamical to simulate the effect of the dynamical stripe-like inhomogeneities, and its time average should maintain the translational symmetry of the CuO_2 planes, as in the bare band in Eq. (19). In the effective system, as in the real one, the stripsons correspond (see Fig. 1) to about a quarter of the relevant orbitals of the Cu atoms in the planes, while the QE's to the remaining three quarters.

Such an effective dynamical potential exists, and it induces an effective (dynamical) SDW, where minigaps are created between the states corresponding to three quarters of the Cu atoms' states, thus blocking their contribution to conductivity at low T and ω , while those corresponding to the remaining quarter of Cu atoms' states continue contributing to conductivity. It also induces a dynamical charge transfer between these two types of Cu atoms. However, this effect is minor since the bare QE and stripon states are strongly renormalized, through the coupling between them [48–50] [see Eq. (2)]. Thus the (dynamical) charge transfer between Cu atoms in the AF and the charged stripes is considerably smaller than what would be concluded from the occupation of stripon and QE states, if they were (wrongly) approximated by their bare states. Such a reduced charge transfer is estimated from the neutron-scattering [23] and STM [27] results.

In the effective system, interband transitions across the minigaps would recover in higher ω and T the contribution to conductivity of the three quarters of the orbitals, blocked at low T and ω , and the f-sum rule would indicate a total number of carriers N_{eff} which is about 4 times the number of (stripon) carriers, contributing to transport at low T and ω . The contribution of carriers residing in the inter-planar layers, discussed above, alters the factor 4 to a somewhat higher factor, but this is partly compensated by the minor (dynamical) charge transfer between planar Cu atoms, mentioned above, and Tanner's law [66] is obtained.

E. Optical carriers in the heavily UD regime

1. Low-energy excitations

An experimental study of the optical conductivity, together with DC transport, for LSCO and YBCO in the heavily UD regime, through x'_0 , x_0 , and the AF phase boundary, was carried out by Padilla *et al.* [67]. Results at low T (7K or just above T_c) and $x < x'_0$ (thus in the regime where transport is dominated by QE's on the nodal FS arcs) show [67] that the Drude term in $\sigma(\omega)$ is fairly separated there from the mid-IR contribution to

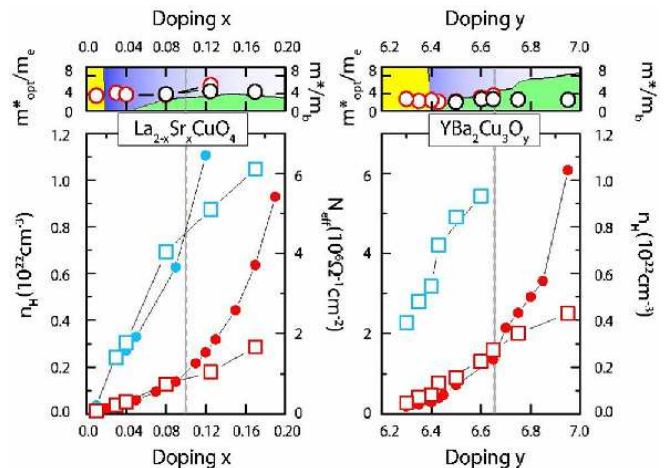


FIG. 5: (Color online) Results presented by Padilla *et al.* [67]. Top panels show the optical effective mass determined by the methods described in the text. Red symbols are the mass determined using a combination of optics and transport (left axis labels), and the black symbols represent the mass determined within the extended Drude model [77, 78] (right labels). The low temperature long range AF ordered phase is denoted by the yellow shaded area and SC region by the green area. Bottom panels show both the effective spectral weight from optics data (red and blue open squares) and the number of holes as determined by transport (red and blue dots).

it. In this case, ω_{co} in the integration in Eq. (22) could be chosen low enough to include, approximately, *only* the Drude term in $\sigma(\omega)$.

Then, similarly to the above analysis of Tanner's law, \mathcal{H} in Eq. (19) could be replaced (in analogy to the Kohn-Sham approach [134]) by an effective Hamiltonian, for which the Drude term would be *the only* contribution to $\sigma(\omega)$, and the effective periodic potential would yield carriers with the effective mass m_{D} of the Drude carriers. Thus, by choosing such ω_{co} , this effective system would yield: $\rho_{\text{D}}/8 = \int_0^{\omega_{\text{co}}} \Re\sigma(\omega)d\omega = \pi n_{\text{D}} e^2 / 2m_{\text{D}}$, where n_{D} is the density of the Drude carriers.

Results obtained by Padilla *et al.* [67] are presented in Fig. 5. The density n_{D} was estimated by measuring the low- T Hall constant (thus assuming $n_{\text{D}} = n_{\text{H}}$), which by Eq. (17), and the discussion following it, corresponds in this regime primarily to the QE's of the nodal FS arcs, as well. The effective mass m_{D} of these carriers was estimated by combining the optical and the Hall results, presented, respectively, by red empty squares and dots in the bottom panels in Fig. 5 (N_{eff} there is $\propto \rho_{\text{D}}$).

The evaluated values of m_{D} are presented as red empty circles in the top panels of Fig. 5, and they turn out [67] to be $\sim 4m_e$ in LSCO, and $\sim 2m_e$ in YBCO, with almost no change over the range $0.01 \lesssim x < x'_0 \simeq 0.09$. The larger mass in LSCO is consistent with the results of Tanner *et al.* [66] discussed above (see Table I). The constant value found for m_{D} in this regime confirms the

GTC scenario that no divergence of the effective mass is occurring for $x \rightarrow 0$ [67], but that carriers are doped within the Hubbard gap, and their density is increasing with doping. These carriers become localized at low T in the low- x regime, and form an FL in the high- x regime. The low- x and high- x limits are separated by the SC phase, or by a QCP in the case that SC is suppressed (see Fig. 3).

Padilla *et al.* [67] found that when x is increased above x'_0 , the overlap between the energy ranges of the Drude and the mid-IR contributions to $\sigma(\omega)$ is growing, and thus the above analysis in terms of a separate Drude term is becoming inappropriate. Nevertheless, a trend can still be observed [67] in Fig. 5 that the low- T ρ_D continues its increase with x at about the same rate as for $x < x'_0$, while the rate of increase of the low- T n_H grows substantially for $x > x'_0$. This may indicate an increase in the effective mass of the carriers for $x > x'_0$, confirming the GTC prediction of a crossover in the type of carriers dominating low- T transport, between QE's on the nodal arcs, and the higher-effective-mass stripons.

2. High-energy excitations

The study by Padilla *et al.* [67] included also the determination of the effective mass m_{eff} , on the basis of a high- ω ρ_{eff} , and a high- T n_{eff} . The first was obtained by integrating on $\Re\sigma(\omega)$ in Eq. (22) up to $\omega_{\text{co}} \simeq 12000 \text{ cm}^{-1}$ (in order to avoid the effect of the ‘‘charge transfer’’ band, as was discussed above [66]). The effective density ($n_{\text{eff}} = n_H$) was obtained by measuring n_H in the high- T Hall-constant plateau, reached at about 800–900 K [67] (thus above T^*). These optical and the Hall results are presented, respectively, by blue empty squares and dots in the bottom panels in Fig. 5 (N_{eff} there is $\propto \rho_{\text{eff}}$). The obtained values [67] of m_{eff} for $x < x'_0$ in LSCO, are about the same as the low- T m_D in this regime, discussed above (presented as red empty circles in the top panels of Fig. 5).

Both the high- T plateau in n_H [see Eq. (17)], and the high- ω ρ_{eff} , in the heavily UD ($x < x'_0$) regime, correspond within the GTC mainly to the contribution of QE's. But while at low T and ω , the QE's determining transport are those on the nodal FS arcs, at high T (above T^*) and ω all the QE's in the conduction band become available for transport, due to the closing of the PG. Thus, the the result: $m_{\text{eff}} \simeq m_D$ [67] indicates that about the same effective mass is relevant for both cases. Temperatures in the 800–900 K range still correspond to a lower energy than that determined by the AF exchange coupling in the cuprates [18, 19], and thus both m_D and m_{eff} are expected to be determined mainly by t' processes [49], which do not compete with the effect of AF exchange.

An analysis of the relation between ρ_{eff} and ρ_D , in the $x < x'_0$ regime, can be carried out similarly to the analysis of Tanner's law above. But here the contribu-

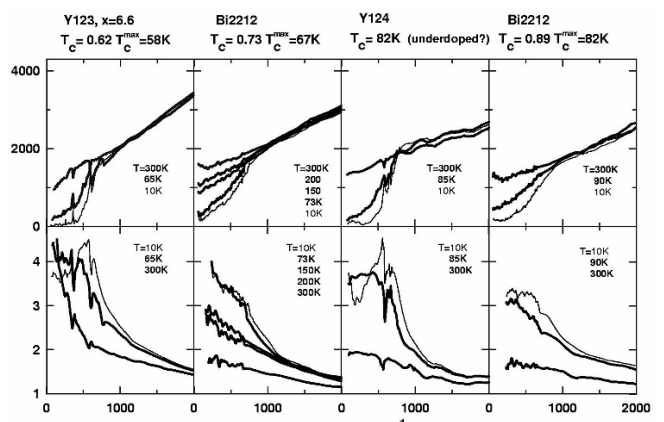


FIG. 6: The frequency dependent scattering rate, top row, and the mass renormalization, bottom row, presented by Puchkov *et al.* [77], for a series of UD cuprate SC's. The scattering rate curves are essentially temperature independent above 1000 cm^{-1} , but develop a depression at low temperature and low frequencies. The effective mass is enhanced at low temperature and low frequencies.

tion of the carriers to transport, except for the QE's on the nodal FS arcs, is blocked, at low T and ω , by (real) gaps, and becomes available when the wide frequencies range is considered. Thus, a different factor is expected for ρ_{eff}/ρ_D in this regime, than the 4-5 factor [66] obtained above in Tanner's law around the OPT regime. And indeed, Padilla *et al.* [67] got $\rho_{\text{eff}}/\rho_D \simeq 6-7$, for $x < x'_0$, and a crossover to Tanner's 4-5 factor, as x is increased above x'_0 , as is expected from the crossover to a stripon-dominated low- T transport in the rest of the doping regime.

Padilla *et al.* [67] also applied the ‘‘extended Drude model’’ [77, 78]:

$$\frac{m^*(\omega)}{m_b} = -\frac{\omega_{\text{pn}}^2}{4\pi\omega} \Im \left[\frac{1}{\sigma(\omega)} \right], \quad (24)$$

$$\omega_{\text{pn}}^2 = \rho_D = \frac{4\pi e^2 n_D}{m_D}, \quad (25)$$

(ω_{pn} is the normal-state plasma frequency) to estimate the mass renormalization $m^*(\omega = 0)/m_b$, in LSCO and YBCO, about room temperature, for x below and above x'_0 . The obtained values are presented as black empty circles in the top panels of Fig. 5. The results for m^*/m_b are close to the values (presented in red-circles) obtained for m_D/m_e for $x < x'_0$, at low T and ω .

As is demonstrated in the bottom row of Fig. 6, for results of Puchkov *et al.* [77] for UD cuprates, such an estimate of m^*/m_b involves an extrapolation to $\omega = 0$ from the mid-IR range, reflecting again a dominant contribution of QE's, both for $x < x'_0$ and $x > x'_0$. Thus the agreement with the effective mass of the QE's on the nodal FS arcs, which are dominant for $x < x'_0$ at low T , is expected. This mass renormalization reflects the omission of the contribution of t processes [49] (which,

unlike t' processes [49] do compete with the effect of AF exchange). Thus the $m^*(\omega)/m_b$ ratio is increased for ω smaller than the energy effect of AF exchange [18, 19], as is seen in Fig. 6. This ratio is greater in LSCO than in YBCO (see Fig. 5) because of the smaller t'/t ratio for LSCO [15].

F. In-gap states

1. Low- T unpaired carriers and their nature

As was discussed after Eq. (7), in the UD regime, where the $\bar{\epsilon}^p(\mathbf{k})^2$ term in Eq. (6) is considerably smaller than the $\Delta^p(\mathbf{k})^2$ term at $T \rightarrow 0$, the Bogoliubov transformation dictates [50] an approximate half filling of the stripon band. Such half filling (namely $n^p = \frac{1}{2}$), corresponds by the TEP results [48] to a lightly OD stoichiometry of $x = x_c \simeq 0.19$. Thus, it was concluded [50] that only a part of the stripions are paired at $T \rightarrow 0$, in the UD regime.

The occupation of stripon states can be regarded as consisting of n^p stripon “particles”, and $(1 - n^p)$ stripon “holes”, per stripon state. The $T \rightarrow 0$ stripon-pairing scenario, within the UD regime, can be approximately described as a situation where each paired stripon “hole” is “coupled” with a stripon “particle” (thus yielding lower and upper Bogoliubov bands, each of approximately equal contributions of stripon “holes” or “particles”). Within this scenario, there are unpaired states of stripon “holes”, which are not “coupled” to stripon “particles”, and *vice versa*.

In p-type cuprates, a linear approximation, expressing the dependence of the number/state of stripon “holes” on x , yields: $1 - n^p \simeq x/2x_c$. Since the $T \rightarrow 0$ number/state of paired stripon “holes” drops from $1 - n^p$, at $x = x_c$, to zero at $x = x_0$, a linear approximation in x would yield for it: $(1 - n^p)(x - x_0)/(x_c - x_0)$. Thus, the $T \rightarrow 0$ number/state of unpaired stripon “holes” would then be approximated as: $(1 - n^p)[1 - (x - x_0)/(x_c - x_0)] = (1 - n^p)(x_c - x)/(x_c - x_0)$.

As was shown in Eq. (16), and the discussion following it, the major contribution to $\sigma_{ab}(\omega)$, for low T and ω , in the OPT and lightly UD regime (corresponding to $x_c > x \gtrsim x_0'' \simeq 0.13$ [67]), is due to stripon “holes”, both above and below T_c . Thus (at low- ω in p-type cuprates in this regime), a density of approximately $n_{\text{con}} \propto (1 - n^p)$ carriers exists in $\sigma_{ab}(\omega)$ just above T_{pair} . At $T \rightarrow 0$, a part n_{prd} of this density is of paired carriers, while the other part, n_{unp} , is of carriers which remain unpaired, and become localized below a temperature T_{loc} . Using

the above linear interpolation in x , one can express:

$$\begin{aligned} n_{\text{con}} &\propto 1 - n^p \simeq \frac{x}{2x_c}, \\ n_{\text{prd}} &\simeq n_{\text{con}} \left(\frac{x - x_0}{x_c - x_0} \right), \\ n_{\text{unp}} &\simeq n_{\text{con}} \left(\frac{x_c - x}{x_c - x_0} \right), \\ 0.13 &\simeq x_0'' \lesssim x < x_c \simeq 0.19. \end{aligned} \quad (26)$$

As was discussed above, the QE contribution to the Drude term in $\sigma_{ab}(\omega)$ (as carriers' density n_{con} above T_{pair} , and n_{unp} below it), and to the δ -function superfluid term in it (as carriers' density n_{prd}), is growing when x is decreased. The relative QE contribution to the Drude term above T_{pair} is growing when T is increased. The low- T unpaired carriers (of density n_{unp}) become dominated by QE's on the nodal FS arcs, for $x < x_0' \simeq 0.09$. The crossover between the regimes of stripon- and QE-dominated low- T transport occurs for $x_0' < x < x_0''$ [67].

The observed behavior [66, 71–73] of the low- ω $\sigma_{ab}(\omega)$ below T_{pair} (both in the SC and PG states) confirms the above predictions. This is viewed in the effect of the n_{unp} unpaired carriers, appearing as a low frequency Drude-like term [66, 71–73] (see Figs. 4, 7, and 8). The width of this Drude term is smaller than that of the normal-state Drude term [66], and it is further decreased [66, 72] when the temperature is decreased, which will be shown below to be a consequence of the GTC. This Drude term turns into a low- ω peak in $\sigma_{ab}(\omega)$ for $T < T_{\text{loc}}$ [66, 72], as is expected for localized carriers. Also the spectral weight within this Drude-like term agrees with the trend predicted in Eq. (26) for n_{unp} , being small for the OPT stoichiometry [66], where x is only a little below x_c , and increasing [72] as x is decreased within the UD regime (see below).

2. The contribution of $\mathbf{j}^{\text{qp}}(\omega)$

Another contribution to $\sigma_{ab}(\omega)$, which is in agreement with the GTC predictions, is the one due to transitions between QE and stripon-svicon states [71–75], and its evolution with T for $0 < T < T_{\text{pair}}$. Since the stripe-like inhomogeneities are generated by the Bose condensation of the svicons, and their structure is determined by the details of the of the svicon spectrum, around its energy minimum (see Fig. 2), attempts to interpret the structure contributed to $\sigma_{ab}(\omega)$ as a signature of stripes [71, 72] are consistent with the present approach. Since the interval of svicon energies involved is between $+\bar{\epsilon}^\zeta(\mathbf{k}_{\text{min}})$ and $-\bar{\epsilon}^\zeta(\mathbf{k}_{\text{min}})$, and thus its width is equal by Eq. (9) to the resonance-mode energy, attempts to interpret the contributed optical structure in terms of spin excitations, and specifically the resonance mode [74, 75], are also consistent with the present approach.

The energies involved in transitions between QE and stripon-svicon states include the energy difference between an occupied QE, and an unoccupied stripon state,

or *vice versa*, plus or minus a svivon energy. As was discussed above, the stripon bandwidth is ~ 0.02 eV, in the normal state, and smaller in a pairing state due to the nature of the expression for Bogoliubov quasiparticle energies, in Eq. (6). The QE's, on the other hand, have a wide energy spectrum around E_F . The svivon spectrum is sketched in Fig. 2; its bottom is ~ 0.02 eV below zero, and its top is few tenths of an eV above zero. So these transitions contribute to $\sigma_{ab}(\omega)$ a wide, almost featureless, spectrum, forming a major part of its mid-IR background [66] (see Fig. 4). An important role in these transitions is played by svivons around their energy minimum at \mathbf{k}_0 where, by Eq. (1), the $\cosh(\xi_{\mathbf{k}})$ and $\sinh(\xi_{\mathbf{k}})$ factors appearing in the scattering Hamiltonian in Eq. (2) are large. As was discussed above, they are excited during transitions between stripions and QE's around the antinodal points.

When the stripon and QE pairing gaps open below T_{pair} , the width of svivon states around their minimum at \mathbf{k}_0 decreases, as was discussed before Eq. (9). In an analogous manner to the spectroscopic results in Eqs. (8) and (9), one gets that transitions between QE states on one side of the pairing gap, and stripon-svivon states on its other side, result in a contribution to $\sigma_{ab}(\omega)$ around the gap-edge energy. This contribution narrows down below T_c to a peak of the width $\gtrsim W_{\text{peak}}$, given in Eq. (9), which equals the resonance-mode energy. Note, however, that in the heavily OD regime, the dispersion in the stripon Bogoliubov band becomes larger than W_{peak} , resulting in the smearing of the peak due to the \mathbf{k} -integration taking place when the optical spectrum is derived. Such a peak of the predicted width has been observed by Hwang *et al.* [75], over a wide range of doping, and was found to “disappear” in the heavily OD regime, which, as predicted above, is due to smearing.

3. Evolution of the states with doping

The existence of unpaired stripon states within the pairing gap, for $x < x_c$, causes (as was discussed above) an increase in the width of this peak above W_{peak} (as is noticed in Ref. [75] in the UD regime). The inclusion of transitions between QE and unpaired stripon-svivon states results in a wider peak in $\sigma_{ab}(\omega)$, centered within the energy range of the optical “gap” [which, as will be discussed below, does not appear as a gap in $\sigma_{ab}(\omega)$]. Furthermore, as was discussed above, the unpaired stripions [see Eq. (26)] introduce also a Drude-like term, turning for $T < T_{\text{loc}}$ into a peak in $\sigma_{ab}(\omega)$, which merges with the one due to transitions between QE and stripon-svivon states into one peak, within the range of the optical “gap”. The appearance of this merged peak could be regarded as a signature of the glassy (checkerboard) structure intertwined with the localization of the stripon carriers, and the creation of an associated gap.

Measurements of the evolution of this structure in $\sigma_{ab}(\omega)$, as T is lowered through T^* and T_c , were pre-

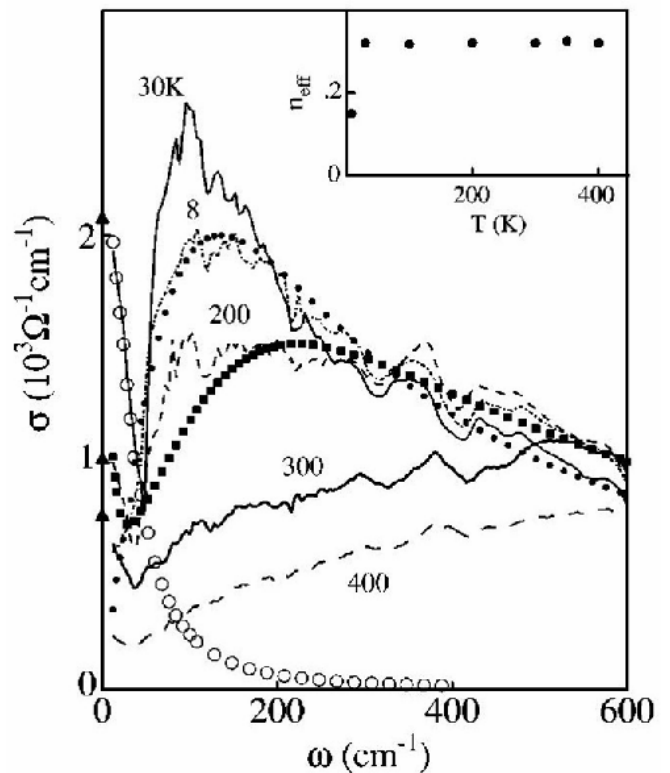


FIG. 7: Far-IR range of $\Re\sigma(\omega)$ of a BSCO film, presented by Lupi *et al.* [71]. The open circles are the best fit to a normal Drude term, here proposed only for the 30 K curve. The dots and squares are best fits to proposed model curves [71] to data at 8 and 200 K, respectively. The triangles on the ordinate axis represent the values of σ_{DC} measured at the same temperatures. The inset shows the spectral weight calculated through the partial f-sum rule.

sented in Refs. [71–73]. The results of Lupi *et al.* [71] on single-layer BSCO are presented in Fig. 7. They show a Drude term at very low energies, due to the density n_{unp} of unpaired carriers below T_{pair} given in Eq. (26). They also show a term due to transitions between QE and stripon-svivon states, which is moved from the mid-IR range, and narrows down, as T is lowered, into a peak overlapping energies within the range of the optical gap, as is suggested above.

The results of Lucarelli *et al.* [72] on LSCO for eight doping levels in the range $0 < x < 0.26$ are presented in Fig. 8. They show a Drude normal behavior for $x = 0.26$, while for $x = 0.19, 0.15$, they show the evolution of a peak due to transitions between QE and stripon-svivon states, similarly to the one shown in Fig. 7 for BSCO [71]. A low-energy Drude term, due unpaired carriers below T_{pair} (as in Fig. 7) is observed in Fig. 8 for $x = 0.15$. Sharp peaks due to phonon modes are observed too. For $x = 0.12$, this Drude term turns (due to localization in the glassy structure) into a peak, merging (as was suggested above) with the other peak (due to transitions between QE and

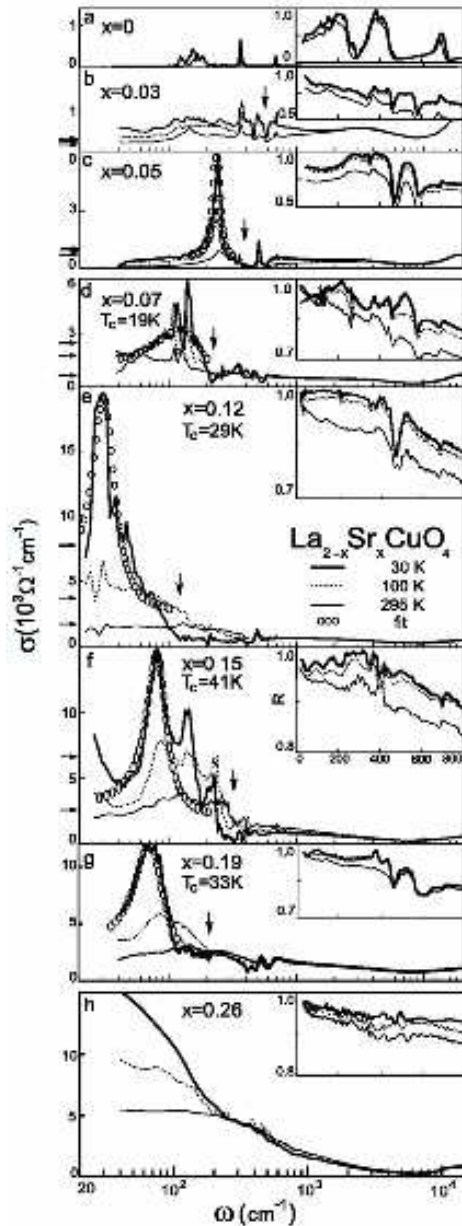


FIG. 8: Optical conductivity in the ab plane, $\Re\sigma_{ab}(\omega)$, presented by Lucarelli *et al.* [72], for $\text{La}_{2-x}\text{Sr}_x\text{CuO}_4$ with increasing hole doping, from top to bottom. Raw reflectivity data are shown in the insets for the far-IR range. Horizontal arrows mark the DC conductivity measured at the same temperature as the spectrum plotted with corresponding symbols. The fits and vertical arrows are explained in Ref. [72].

stripon–svivon states), and the center of the combined peak shifts to lower energy. A similar low- T merged peak, within the SC optical gap, is observed also in Fig. 4 [66].

For $x = 0.07$ and $x = 0.05$ [72] this peak in Fig. 8 shifts to a higher energy, with the decrease of x , which is consistent with the increase of the localization gap. This peak turns into a wider background for $x = 0.03$ [72], consis-

tently with the change of the structure into that of diagonal stripes, and it almost disappears for $x = 0$. Padilla *et al.* [135] studied the evolution of this structure, and the phonon modes in it, in the range $0 \leq x \leq 0.08$, where x passes through $x_0 \simeq 0.05$. Lee *et al.* [136] found a similar behavior in the very low doping regime in YBCO.

Kim *et al.* [73] studied LSCO for $x = 0.11, 0.09, 0.07, 0.063$, and also obtained in this regime a combined peak, as in Fig. 8 (interpreted here to be related to the glassy structure), which is shifting to a higher energy, with the decrease of x . At $T = 300\text{K}$ [73] they extrapolated a low-energy Drude term, due to the contribution of QE’s on the nodal FS arcs, discussed above [67]. This Drude term is of a different nature than that due to the stripon contribution to n_{unp} [given in Eq. (26)], which is observed at higher values of x .

V. OPTICAL CONDUCTIVITY IN THE c DIRECTION

Optical conductivity out of the CuO_2 planes, and specifically in the c direction, cannot be discussed within the one-band Hamiltonian of Eq. (19), and inter-planar orbitals are involved. The normal-state DC conductivity in the c direction is coherent in cases like OD YBCO [137], due to the chains orbitals, and incoherent in other cases. SC in the c direction has been often attributed [138–140] to Josephson tunneling between the CuO_2 planes [141, 142]. This scenario is *not* distinct from the description of the c -direction SC as bulk SC within the dirty limit. Both scenarios give the same temperature dependence of the c -direction penetration depth [138, 139].

The inter-planar layers may be too thin to be described as “metallic” or “insulating”. Since the orbitals of the SC electrons of the CuO_2 planes are hybridized with inter-planar orbitals, the Cooper pairs of the planes do penetrate the inter-planar layers, and in cases that these layers contribute many carriers around E_F , proximity-induced pairing is expected to exist there [8]. Upon crossing to the OD regime [137], coherence in c direction can be established in the normal state, and the dirty-limit scenario looks more natural than the Josephson scenario, but still the c -direction SC features are not significantly altered.

The SC transition is followed by the establishment of a c -direction SC plasmon mode [56, 92, 143], which is referred to, within the Josephson tunneling scenario, as a Josephson plasma resonance. But it is also expected within the GTC pairing mechanism, discussed above [49], due to the hybridization of orbitals of the inter-planar layers with the CuO_2 -plane QE states, resulting in some inter-plane pair hopping. Effects of the SC transition on the c -direction optical conductivity include a similar “violation” of the f–sum rule [57, 63], as in the ab -plane optical conductivity, due to transfer of spectral weight from energies $\gtrsim 2\text{eV}$, which was explained above within the GTC.

Another c -direction optical effect is the transfer of spectral weight from the SC gap to the mid- or far-IR range, which has been identified [56, 61–65] as the signature of a c -axis collective mode. In bilayer structures it was attributed to a transverse out-of-phase bilayer plasmon, related to “excitons” first considered by Leggett [145], due to relative phase fluctuations of the condensates formed in two different bands. The observation of a similar effect in monolayer LSCO [63] suggests that the LaSrO layers, where the doped atoms reside, may introduce enough states close to E_F to provide the second band needed for such transverse plasmons to be formed. This collective mode was found [63, 65] to be well defined already in the PG state. This is consistent with the GTC under which the pairs already exist in this state, and even though they lack long-range phase coherence, short-range effects over the distance between close planes/layers, required for this mode to exist, are expected to be present.

VI. OPTICAL SCATTERING RATES

Using the extended Drude model [77, 78], the optical scattering rate can be expressed as [see Eq. (25)]:

$$\frac{1}{\tau(\omega)} = \frac{\omega_{\text{pn}}^2}{4\pi} \Re \left[\frac{1}{\sigma(\omega)} \right] \quad (27)$$

(thus the carriers density dependence of the conductivity is eliminated to obtain the scattering rate). The ab -plane and c -direction scattering rates, $\tau_{ab}(\omega)^{-1}$ and $\tau_c(\omega)^{-1}$, behave differently in the cuprates. Quantum criticality [81] close to the QCP in the normal state (see Fig. 3) results in the existence of a critical region where only one energy scale, which is the temperature, exists. Consequently an MFL-type behavior [5] is obtained there (thus linearity in ω) for $\tau_{ab}(\omega)^{-1}$ and related quantities [80], and further optical quantities behave critically [81].

As was shown in Eq. (16), and the discussion following it, the conductivity in the ab plane, $\sigma_{ab}(\omega)$, is dominantly stripon-like for low T and ω for $x > x_0''$ [see Eq. (26)]. Consequently, $\tau_{ab}(\omega)^{-1}$ is determined in this regime by the scattering of stripions, through \mathcal{H}' [see Eq. (2)] into QE and svivon states [48, 49]. As was discussed before Eq. (9), the main contribution to such scattering comes [50] from QE states around the antinodal points, and svivon states around their energy minimum at \mathbf{k}_0 (see Fig. 2), where, by Eq. (1), the $\cosh(\xi_{\mathbf{k}})$ and $\sinh(\xi_{\mathbf{k}})$ factors are large. Below T_{pair} a QE pairing gap opens around the antinodal points, and as was discussed above, all the QE states there either become paired, or have a localization gap, for $T \rightarrow 0$. This results in a reduction, below T_{pair} , of $\tau_{ab}(\omega)^{-1}$, for ω within the pairing gap. This reduction becomes drastic at low T , when the width of the gap-edge peak becomes small (because of the exclusion of such scattering), and the QE gap approaches its $T \rightarrow 0$ value.

Since the width of the Drude term in $\sigma_{ab}(\omega)$ is τ_{ab}^{-1} , its decrease below T_{pair} results in a smaller Drude width for

the unpaired carriers there [see Eq. (26) and the above discussion], than for the carriers above T_{pair} (see Fig. 4). Furthermore, this Drude width is expected to decrease with decreasing temperature, in agreement with experiment [66, 72]. As was discussed above, the relative contribution of QE’s to the Drude term is growing when T is increasing above T_{pair} . This results in an increase in the width τ_{ab}^{-1} of the Drude term with T above T_{pair} , in agreement with experiment [66] (see Fig. 4).

For $x < x_0''$, the nature of the unpaired carriers below T_{pair} crosses over from being dominantly stripon like, to being dominated by QE’s on the nodal FS arcs. However, this does *not* result in an increase in their scattering rate τ_{ab}^{-1} (and thus Drude width), because (unlike the antinodal QE’s, which contribute significantly above T_{pair}) these QE’s are not scattered to stripon–svivon states, around the svivons’ energy minimum at \mathbf{k}_0 (see Fig. 2), and the contribution of other svivons to their scattering is much smaller (as was discussed above). And indeed, the width of the Drude term in the heavily UD regime was found [67] to be pretty small and even fairly separated from the mid-IR term, as was discussed above.

A consequence of the existence of unpaired carriers within the gap is that the drop in τ_{ab}^{-1} below T_{pair} is not followed by an equal relative drop in the effective density of carriers. Since these carriers contribute to DC conduction for $T > T_{\text{loc}}$, the expected effect is an *increase* in the ab -plane DC conductivity above T_{loc} in the PG state. This explains the observed [85] sublinear T -dependence of the DC resistivity for $T_{\text{loc}} < T < T^*$ in the UD regime. Also is explained the increase in this effect on the resistivity [85] when x is decreased, and thus T^* and the PG size are increased.

The c -direction conductivity $\sigma_c(\omega)$ is, on the other hand, determined by the QE states (with hybridization taking place between planar states and inter-planar orbitals). Thus $\tau_c(\omega)^{-1}$ is determined by scattering of QE’s to stripon–svivon states, persisting below T_c (and thus resulting in the wide hump, as was discussed above), and by processes within the inter-planar layers, which are unrelated to the pairing process, and it is not expected to vary significantly below T_{pair} . Since and the number of unpaired QE’s drops below T_{pair} (while τ_c^{-1} does not vary significantly), a drop in $\sigma_c(\omega)$ within the gap is occurring below T_{pair} . The contribution to it from pairs is expected to be transferred to the δ -function term in the SC state, and to higher frequencies in the PG state, where the pairs are localized.

The contribution of the QE localization gaps to the PG (discussed above), especially in the heavily UD regime, also contributes to the drop in $\sigma_c(\omega)$ within the gap. The spectral weight corresponding to these localized states is not transferred to the δ -function term, when the localization gaps (approximately) exceed the pairing gaps, and this applies to most of the QE’s when $x \rightarrow x_0$.

These predictions are confirmed by experiment. A sharp drop has been observed [77, 79] in $\tau_{ab}(\omega)^{-1}$ of the quasiparticles below T_c , as can be seen in the top row of

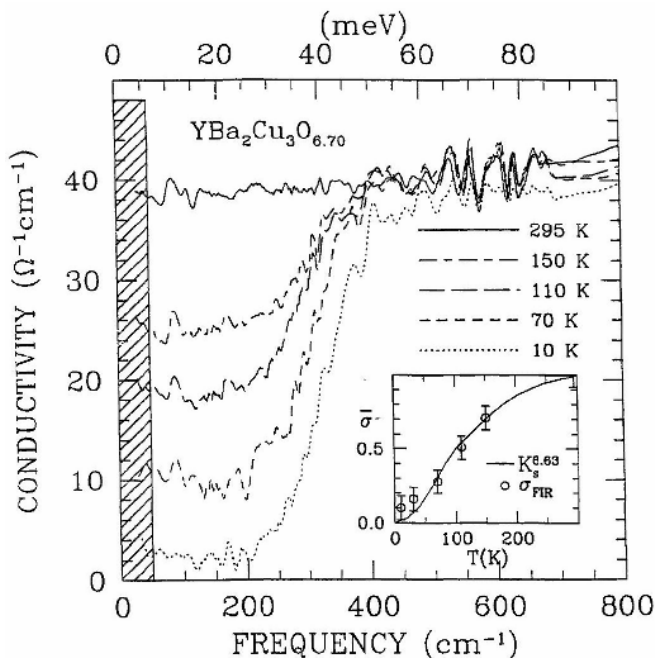


FIG. 9: The c -axis optical conductivity $\Re\sigma_c(\omega)$ of a UD Y123 crystal, presented by Puchkov *et al.* [77]. The c -axis conductivity is temperature and frequency independent for $T > T^*$, but develops a marked gap-like depression below T^* . As the temperature is lowered the PG deepens. Inset: the NMR Knight shift (normalized at 300 K) is plotted as a function of temperature for a UD Y123 crystal. The circles show the low-frequency c -axis conductivity for samples of the same doping level. The curves suggest that the Knight shift, a conventional measure of the DOS at E_F , and the c -axis conductivity are depressed by the same process in the PG state.

Fig. 6. Consequently a clean-limit treatment applies in the SC state within the ab plane, while $\tau_{ab}(\omega)^{-1}$ above T_c corresponds to the intermediate scattering regime (see below) [146]. Also, as can be seen in Fig. 6, the reduction in $\tau_{ab}(\omega)^{-1}$, for ω within the gap, starts in the PG state (thus below $T^* = T_{\text{pair}}$) [77, 78].

On the other hand, as can be seen in Fig. 9, a gap-like depression has been observed below T^* [76, 77] in $\sigma_c(\omega)$ within the PG energy range, with the spectral weight from it transferred to higher energies (above T_c). The similarity, shown in the inset in Fig. 9, between the gap-like behavior in $\sigma_c(\omega \rightarrow 0)$, and the gap observed in Knight-shift results, is consistent with the GTC prediction that this gap is in the spectrum of spin-carrying QE-like carriers.

VII. HOMES' LAW

Homes *et al.* [83] have demonstrated that, in many SC's, the optical quantity $\rho_s = \omega_{\text{ps}}^2$ [based on a similar expression as in Eq. (4)], obeys approximately (thus when

presented on a log-log scale) the relation

$$\rho_s \simeq 35\sigma_{\text{DC}}(T_c)T_c \quad (28)$$

(both sides in the equation possess the same units). This relation, known as Homes' law, is obeyed in the cuprates in almost the entire doping regime, both in the ab -plane, and in the c -direction, and in other SC's which behave according to dirty-limit approximations. In a subsequent paper, Homes *et al.* [146] demonstrated that this law should be valid in the dirty-limit, and in the intermediate-scattering regime, when it applies to transport in the *normal state*. The reason is that the $\rho_s/8$ spectral weight, which condenses into the superfluid δ -function term in $\sigma(\omega)$, approximately scales then as the product of $\sigma_{\text{DC}}(T_c)$ and the SC gap, which approximately scales as T_c . Thus, in the regime of validity of Homes' law, it could be expressed as:

$$k_B T_c \lesssim \hbar\tau^{-1}(T_c), \quad (29)$$

As was discussed above, $\sigma_{ab}(\omega)$ in the cuprates corresponds to the intermediate-scattering regime in the normal state, with most of the Drude carriers turning into a superfluid. But the drop in $\tau_{ab}(\omega)$ below T_c (seen in Fig. 6), predicted by the GTC, turns them into clean-limit SC's. The c -direction conductivity was discussed above as being described by the dirty-limit both above and below T_c , and also through the Josephson tunneling scenario, which was shown [83, 137] to result in Eq. (28) too. Thus, the GTC is consistent with the applicability of Homes' law in the cuprates, both in the ab -plane, and the c -direction, and it could be expressed there as:

$$k_B T_c(\text{cuprates}) \simeq \hbar\tau^{-1}(T_c). \quad (30)$$

This expression is the consequence of the MFL behavior [5], due to quantum criticality, and thus [81] the existence of one energy scale, which is the temperature. The coexistence of Homes' law with Uemura's law [see Eq. (4)] in the UD regime implies, by Eq. (28), that $\sigma_{\text{DC}}(T_c)$ does not vary much with x there (in agreement with experiment [85], except when localization starts above T_c), which was shown above to be the consequence of the decrease in τ_{ab}^{-1} [and by Eq. (30), also in T_c] in the PG state.

Eq. (30) connects high T_c in the cuprates with a high scattering rate, which lead also to an MIT. The existence of SC close to the boundary of MIT's has been pointed out by Osofsky *et al.* [147]. Zaanen [84] suggested that Homes' law implies that T_c in the cuprates is determined, approximately by the condition that the scattering rate in the normal state is becoming at T_c as high as is permitted by the laws of quantum physics. Here it was shown that the high scattering rate is strongly decreased below T_c , since it is determined by the same interactions which determine pairing.

VIII. CONCLUSIONS

The success of the GTC in providing the understanding of a variety of puzzling optical properties of the cuprates, in addition to its earlier success in explaining many other anomalous properties of these materials, strengthens the point of view that the occurrence of high- T_c SC in them requires the proximity of a Mott transition.

It suggests the occurrence of spin-charge separation in the cuprates [3], *but* only due to the existence of dynamical inhomogeneities, which provide quasi-one-dimensional structures. It also predicts an intrinsic origin to the static nanoscale heterogeneity observed in the UD

regime [28].

Furthermore, the GTC supports the opinion that the same interactions which play a major role in the determination of the electronic structure of the cuprates, also primarily determine pairing, transport, and other anomalous properties in them.

Even though a complete rigorous first-principles proof on the validity of the GTC is still beyond reach, due to the complexity of the global scheme, and many of its results are still obtained on a qualitative level, the mounting evidence on the global scope of its applicability points very strongly to its validity for the cuprates.

-
- [1] J. G. Bednorz, and K. A. Müller, *Z. Phys. B* **64**, 189 (1986).
- [2] Peter Brusov, *Mechanisms of High Temperature Superconductivity I & II* (Rostov State University Publishing, 1999).
- [3] P. W. Anderson, *Phys. Rev. Lett.* **64**, 1839 (1990).
- [4] Bogdan A. Bernevig, Robert B. Laughlin, and David I. Santiago, *Phys. Rev. Lett.* **91**, 147003 (2003).
- [5] C. M. Varma P. B. Littlewood, S. Schmitt-Rink, E. Abrahams and A. E. Ruckenstein, *Phys. Rev. Lett.* **63**, 1996 (1989).
- [6] Patrick A. Lee, Naoto Nagaosa, Xiao-Gang Wen, <http://aps.arxiv.org/abs/cond-mat/0410445>.
- [7] V. J. Emery, and S. A. Kivelson, *Nature* **374**, 434 (1995); *Phys. Rev. Lett.* **74**, 3253 (1995); <http://aps.arxiv.org/abs/cond-mat/9710059>.
- [8] V. Z. Kresin, S. A. Wolf, and G. Deutscher, *Physica C* **191**, 9 (1992); V. Z. Kresin, and S. A. Wolf, *Physica C* **198**, 328 (1992).
- [9] Sudip Chakravarty, R. B. Laughlin, Dirk K. Morr, and Chetan Nayak, *Phys. Rev. B* **63**, 094503 (2001).
- [10] C. M. Varma, *Phys. Rev. B* **55**, 14554 (1997).
- [11] Annette Bussmann-Holder, K. Alex Müller, Roman Micnas, Helmut Buttner, Arndt Simon, Alan R. Bishop, and Takeshi Egami *J. Phys.: Condens. Matter*, **13**, L168 (2001); Annette Bussmann-Holder, Alan R. Bishop, Helmut Buttner, Takeshi Egami, Roman Micnas, and K. Alex Müller, **13**, L545 (2001).
- [12] D. Mihailovic and V. V. Kabanov, *Phys. Rev. B* **63**, 054505 (2001); V. V. Kabanov and D. Mihailovic, *Phys. Rev. B* **65**, 212508 (2002).
- [13] B. V. Fine, *Phys. Rev. B* **70**, 224508 (2004).
- [14] Warren E. Pickett, *Rev. Mod. Phys.* **61**, 433 (1989).
- [15] E. Pavarini, I. Dasgupta, T. Saha-Dasgupta, O. Jepsen, and O. K. Andersen, *Phys. Rev. Lett.* **87**, 047003 (2001).
- [16] R. S. Markiewicz, S. Sahrakorpi, M. Lindroos, Hsin Lin, and A. Bansil, <http://aps.arxiv.org/abs/cond-mat/0503064>.
- [17] A. Macridin, M. Jarrell, Th. Maier, and G. A. Sawatzky, *Phys. Rev. B* **71**, 134527 (2005).
- [18] V. I. Anisimov, M. A. Korotin, I. A. Nekrasov, Z. V. Pchelkina, and S. Sorella, *Phys. Rev. B* **66**, 100502 (2002).
- [19] David Muñoz, Ibério de P.R. Moreira, and Francesc Illas, *Phys. Rev. B* **71**, 172505 (2005).
- [20] R. J. McQueeney, J. L. Sarrao, P. G. Pagliuso, P. W. Stephens, and R. Osborn, *Phys. Rev. Lett.* **87**, 077001 (2001); J.-H. Chung, T. Egami, R. J. McQueeney, M. Yethiraj, M. Arai, T. Yokoo, Y. Petrov, H. A. Mook, Y. Endoh, S. Tajima, C. Frost, and F. Dogan, *Phys. Rev. B* **67**, 014517 (2003); L. Pintschoius, Y. Endoh, D. Reznik, H. Hiraka, J. M. Tranquada, W. Reichardt, H. Uchiyama, T. Masui, and S. Tajima, <http://aps.arxiv.org/abs/cond-mat/0308357>; T. Cuk, F. Baumberger, D. H. Lu, N. Ingle, X. J. Zhou, H. Eisaki, N. Kaneko, Z. Hussain, T. P. Devereaux, N. Nagaosa, and Z.-X. Shen, <http://aps.arxiv.org/abs/cond-mat/0403521>; T. P. Devereaux, T. Cuk, Z.-X. Shen, and N. Nagaosa, <http://aps.arxiv.org/abs/cond-mat/0409426>.
- [21] G.-H. Gweon, T. Sasagawa, S. Y. Zhou, J. Graf, H. Takagi, D.-H. Lee, and A. Lanzara, *Nature* **430**, 187 (2004); A. Lanzara, G.-H. Gweon, and S. Y. Zhou, in *New Challenges in Superconductivity: Experimental Advances and Emerging Theories*, edited by J. Ashkenazi, M. V. Eremin, J. L. Cohn, I. Eremin, D. Manske, D. Pavuna, and F. Zuo (Springer, 2005), p. 1.
- [22] A. Bianconi, N. L. Saini, T. Rossetti, A. Lanzara, A. Perali, M. Messori, H. Oyanagi, H. Yamaguchi, Y. Nishihara, and D. H. Ha, *Phys. Rev. B* **54**, 12018 (1996).
- [23] J. M. Tranquada, J. D. Axe, N. Ichikawa, Y. Nakamura, S. Uchida, and B. Nachumi, *Phys. Rev. B* **54**, 7489 (1996); J. M. Tranquada, J. D. Axe, N. Ichikawa, A. R. Moodenbaugh, Y. Nakamura, and S. Uchida, *Phys. Rev. Lett.* **78**, 338 (1997).
- [24] A. Shengelaya, M. Bruun, B. I. Kochelaev, A. Safina, K. Conder, and K. A. Müller, *Phys. Rev. Lett.* **93**, 017001 (2004).
- [25] L. P. Gor'kov, and G. B. Teitelbaum, in *New Challenges in Superconductivity: Experimental Advances and Emerging Theories*, edited by J. Ashkenazi, M. V. Eremin, J. L. Cohn, I. Eremin, D. Manske, D. Pavuna, and F. Zuo (Springer, 2005), p. 55, <http://aps.arxiv.org/abs/cond-mat/0402589>.
- [26] C. Howald, H. Eisaki, N. Kaneko, M. Greven, and A. Kapitulnik, *Phys. Rev. B* **67**, 014533 (2003); A. Fang, C. Howald, N. Kaneko, M. Greven, and A. Kapitulnik, *Phys. Rev. B* **70**, 214514 (2004).
- [27] T. Hanaguri, C. Lupien, Y. Kohsaka, D.-H. Lee, M. Azuma, M. Takano, H. Takagi, and J. C. Davis,

- Nature* **430**, 1001 (2004).
- [28] K. McElroy, R. W. Simmonds, J. E. Hoffman, D.-H. Lee, J. Orenstein, H. Eisaki, S. Uchida, and J. C. Davis, *Nature* **422**, 592 (2003); K. McElroy, D.-H. Lee, J. E. Hoffman, K. M. Lang, J. Lee, E. W. Hudson, H. Eisaki, S. Uchida, and J. C. Davis, *Phys. Rev. Lett.* **94**, 197005 (2005); K. McElroy, D.-H. Lee, J. E. Hoffman, K. M. Lang, E. W. Hudson, H. Eisaki, S. Uchida, J. Lee, and J. C. Davis, <http://aps.arxiv.org/abs/cond-mat/0404005>.
- [29] J. Zaanen, and O. Gunnarsson, *Phys. Rev. B* **40**, 7391 (1989).
- [30] K. Machida, *Physica C* **158**, 192 (1989).
- [31] V. J. Emery, and S. A. Kivelson, *Physica C* **209**, 597 (1993).
- [32] F. Bucci, C. Castellani, C. Di Castro, and M. Grilli, *Phys. Rev. B* **52**, 6880 (1995).
- [33] H. Won, and K. Maki, *Phys. Rev. B* **49**, 1397 (1994).
- [34] E. Dagotto, *Rev. Mod. Phys.* **66**, 763 (1994).
- [35] F. F. Assaad, M. Imada, and D. J. Scalapino, *Phys. Rev. B* **56**, 15001 (1997).
- [36] Ehud Altman and Assa Auerbach, *Phys. Rev. B* **65**, 104508 (2002).
- [37] M. R. Norman, and C. Pepin, *Phys. Rev. B* **66**, 100506 (2002).
- [38] T. Eckl, W. Hanke, and E. Arrigoni, *Phys. Rev. B* **68**, 014505 (2003).
- [39] E. Schachinger, and J. P. Carbotte, <http://aps.arxiv.org/abs/cond-mat/0506354>.
- [40] Marcus Fleck, Alexander I. Lichtenstein, and Andrzej M. Oles, *Phys. Rev. B* **64**, 134528 (2001).
- [41] V. I. Anisimov, M. A. Korotin, A. S. Mylnikova, A. V. Kozhevnikov, Dm. M. Korotin, and J. Lorenzana, *Phys. Rev. B* **70**, 172501 (2004).
- [42] M. M. Korshunov, and S. G. Ovchinnikov, *Phys. Solid State* **45**, 1415 (2003).
- [43] N. Hasselmann, A. H. Castro Neto, and C. Morais Smith, *Phys. Rev. B* **69**, 014424 (2004).
- [44] I. Eremin, O. Kamaev, and M. V. Eremin, *Phys. Rev. B* **69**, 094517 (2004).
- [45] I. Eremin, and D. Manske, *Phys. Rev. Lett.* **94**, 067006 (2005); I. Eremin, D. K. Morr, A. V. Chubukov, K. H. Bennemann, and M. R. Norman, *Phys. Rev. Lett.* **94**, 147001 (2005).
- [46] T. Mertelj, V. V. Kabanov, and D. Mihailovic, *Phys. Rev. Lett.* **94**, 147003 (2005).
- [47] R. S. Markiewicz, *Phys. Rev. B* **71**, 220504 (2005).
- [48] J. Ashkenazi, *J. Phys. Chem. Solids*, **63**, 2277 (2002), <http://aps.arxiv.org/abs/cond-mat/0108383>, and references therein.
- [49] J. Ashkenazi, *J. Phys. Chem. Solids*, **65**, 1461 (2004), <http://aps.arxiv.org/abs/cond-mat/0308153>, and references therein.
- [50] J. Ashkenazi, in *New Challenges in Superconductivity: Experimental Advances and Emerging Theories*, edited by J. Ashkenazi, M. V. Eremin, J. L. Cohn, I. Eremin, D. Manske, D. Pavuna, and F. Zuo (Springer, 2005), p. 187, <http://aps.arxiv.org/abs/cond-mat/0407175>, and references therein.
- [51] G. S. Boebinger, Yoichi Ando, A. Passner, T. Kimura, M. Okuya, J. Shimoyama, K. Kishio, K. Tamasaku, N. Ichikawa, and S. Uchida, *Phys. Rev. Lett.* **77**, 5417 (1996).
- [52] J. L. Tallon, and J. W. Loram, *Physica C* **349**, 53 (2001); C. Panagopoulos, A. P. Petrovic, A. D. Hillier, J. L. Tallon, C. A. Scott, and B. D. Rainford, *Phys. Rev. B* **69**, 144510 (2004); S. H. Naqib, J. R. Cooper, J. L. Tallon, R. S. Islam, and R. A. Chakalov, *Phys. Rev. B* **71**, 054502 (2005); S. H. Naqib, J. R. Cooper, R. S. Islam, and J. L. Tallon, *Phys. Rev. B* **71**, 184510 (2005).
- [53] I. Bozovic, G. Logvenov, M. A. J. Verhoeven, P. Caputo, E. Goldobin, and M. R. Beasley, *Phys. Rev. Lett.* **93**, 157002 (2004).
- [54] R. Kubo, *J. Phys. Soc. Japan* **12**, 570 (1957).
- [55] M. Tinkham, and R. A. Ferrel, *Phys. Rev. Lett.* **2**, 331 (1959).
- [56] D. van der Marel, in *Strong Interactions in Low Dimensions* (Physics and Chemistry of Materials with Low Dimensional Structures), edited by D. Baeriswyl, and L. Degiorgi, <http://aps.arxiv.org/abs/cond-mat/0301506>.
- [57] D. N. Basov, C. C. Homes, E. J. Singley, M. Strongin, T. Timusk, G. Blumberg, and D. van der Marel, *Phys. Rev. B* **63**, 134514 (2001).
- [58] H. J. A. Molegraaf, C. Presura, D. van der Marel, P. H. Kes, and M. Li, *Science* **295**, 2239 (2002).
- [59] A. F. Santander-Syro, R.P.S.M. Lobo, N. Bontemps, W. Lopera, D. Giratá, Z. Konstantinovic, Z. Z. Li, and H. Raffy, *Phys. Rev. B* **70**, 134504 (2004).
- [60] C. C. Homes, S. V. Dordevic, D. A. Bonn, Ruixing Liang, and W. N. Hardy, *Phys. Rev. B* **69**, 024514 (2004).
- [61] M. Gruninger, D. van der Marel, A. A. Tsvetkov, and A. Erb, *Phys. Rev. Lett.* **84**, 1575 (2000).
- [62] Diana Dulic, A. Pimenov, D. van der Marel, D. M. Broun Saeid Kamal, W. N. Hardy, A. A. Tsvetkov, I. M. Sutjaha, Ruixing Liang, A. A. Menovsky, A. Loidl, and S. S. Saxena, *Phys. Rev. Lett.* **86**, 4144 (2001).
- [63] A. B. Kuzmenko, N. Tombros, H. J. A. Molegraaf, M. Gruninger, D. van der Marel, and S. Uchida, *Phys. Rev. Lett.* **91**, 037004 (2003).
- [64] D. van der Marel, <http://aps.arxiv.org/abs/cond-mat/0410473>.
- [65] S. V. Dordevic, E. J. Singley, J. H. Kim, M. B. Maple, Seiki Komiya, S. Ono, Yoichi Ando, T. Room, Ruixing Liang, D. A. Bonn, W. N. Hardy, J. P. Carbotte, C. C. Homes, M. Strongin, and D. N. Basov, *Phys. Rev. B* **69**, 094511 (2004).
- [66] D. B. Tanner, H. L. Liu, M. A. Quijada, A. M. Zibold, H. Berger, R. J. Kelley, M. Onellion, F. C. Chou, D. C. Johnston, J. P. Rice, D. M. Ginsberg, and J. T. Markert, *Physica B* **244**, 1 (1998).
- [67] W. J. Padilla, Y. S. Lee, M. Dumm, G. Blumberg, S. Ono, Kouji Segawa, Seiki Komiya, Yoichi Ando, and D. N. Basov, *Preprint* (2005).
- [68] S. Tajima, Y. Fudamoto, T. Kakeshita, B. Gorshunov, V. Zelezny, K. M. Kojima, M. Dressel, and S. Uchida, *Phys. Rev. B* **71**, 094508 (2005).
- [69] Ch. Niedermayer, C. Bernhard, U. Binninger, H. Gluckler, J. L. Tallon, E. J. Ansaldo, and J. I. Budnick, *Phys. Rev. Lett.* **71**, 1764 (1993).
- [70] T. Timusk, private communication.
- [71] S. Lupi, P. Calvani, M. Capizzi, and P. Roy, *Phys. Rev. B* **62**, 12418 (2000).
- [72] A. Lucarelli, S. Lupi, M. Ortolani, P. Calvani, P. Maselli, M. Capizzi, P. Giura, H. Eisaki, N. Kiku-

- gawa, T. Fujita, M. Fujita, and K. Yamada, *Phys. Rev. Lett.* **90**, 037002 (2003).
- [73] Y. H. Kim, P. H. Hor, X. L. Dong, F. Zhou, Z. X. Zhao, Y. S. Song, and W. X. Ti, *J. Phys.: Condens. Matter*, **15**, 8485 (2003).
- [74] J. P. Carbotte, E. Schachinger, D. N. Basov, *Nature* **401**, 354 (1999); E. Schachinger, and J. P. Carbotte, *Phys. Rev. B* **62**, 9054 (2000).
- [75] J. Hwang, T. Timusk, G. D. Gu, *Nature* **427**, 714 (2004).
- [76] C. C. Homes, T. Timusk, R. Liang, D. A. Bonn, and W. N. Hardy, *Phys. Rev. Lett.* **71**, 1645 (1993).
- [77] A. V. Puchkov, D. N. Basov, and T. Timusk, *J. Phys.: Condens. Matter*, **8**, 10049 (1996).
- [78] D. N. Basov, E. J. Singley, and S. V. Dordevic, *Phys. Rev. B* **65**, 054516 (2002); T. Timusk, <http://aps.arxiv.org/abs/cond-mat/0303383>.
- [79] D. A. Bonn, Ruixing Liang, T. M. Riseman, D. J. Baar, D. C. Morgan, Kuan Zhang, P. Dosanjh, T. L. Duty, A. MacFarlane, G. D. Morris, J. H. Brewer, W. N. Hardy, C. Kallin and A. J. Berlinsky, *Phys. Rev. B* **47**, 11314 (1993).
- [80] J. Hwang, T. Timusk, A. V. Puchkov, N. L. Wang, G. D. Gu, C. C. Homes, J. J. Tu, and H. Eisaki, *Phys. Rev. B* **69**, 094520 (2004).
- [81] D. van der Marel, H. J. A. Molegraaf, J. Zaanen, Z. Nussinov, F. Carbone, A. Damascelli, H. Eisaki, M. Greven, P. H. Kes, M. Li, *Nature* **425**, 271 (2003).
- [82] Y. J. Uemura, G. M. Luke, B. J. Sternlieb, J. H. Brewer, J. F. Carolan, W. N. Hardy, R. Kadono, J. R. Kempton, R. F. Kiefl, S. R. Kreitzman, P. Mulhern, T. M. Rise-man, D. Ll. Williams, B. X. Yang, S. Uchida, H. Takagi, J. Gopalakrishnan, A. W. Sleight, M. A. Subramanian, C. L. Chien, M. Z. Cieplak, Gang Xiao, V. Y. Lee, B. W. Statt, C. E. Stronach, W. J. Kossler, and X. H. Yu, *Phys. Rev. Lett.* **62**, 2317 (1989).
- [83] C. C. Homes, S. V. Dordevic, M. Strongin, D. A. Bonn, Ruixing Liang, W. N. Hardy, Seiki Komiya, Yoichi Ando, G. Yu, N. Kaneko, X. Zhao, M. Greven, D. N. Basov, and T. Timusk, *Nature* **430**, 539 (2004).
- [84] Jan Zaanen, *Nature* **430**, 512 (2004).
- [85] H. Takagi, B. Batlogg, H. L. Kao, J. Kwo, R. J. Cava, J. J. Krajewski, and W. F. Peck, Jr., *Phys. Rev. Lett.* **69**, 2975 (1992).
- [86] Yuri Zuev, Mun Seog Kim, Thomas R. Lemberger, <http://aps.arxiv.org/abs/cond-mat/0410135>.
- [87] S. E. Barnes, *Adv. Phys.* **30**, 801-938 (1981).
- [88] J. Ashkenazi, *J. Supercond.* **7**, 719 (1994).
- [89] J. Ashkenazi, in *High-Temperature Superconductivity*, edited by S. E. Barnes, J. Ashkenazi, J. L. Cohn, and F. Zuo (AIP Conference Proceedings 483, 1999), p. 12, <http://aps.arxiv.org/abs/cond-mat/9905172>.
- [90] A. G. Sun, A. Truscott, A. S. Katz, R. C. Dynes, B. W. Veal and C. Gu, *Phys. Rev. B* **54**, 6734 (1996).
- [91] M. Abrecht, D. Ariosa, D. Cloetta, S. Mitrovic, M. Onellion, X. X. Xi, G. Margaritondo, and D. Pavuna, *Phys. Rev. Lett.* **91**, 057002 (2003).
- [92] S. V. Dordevic, Seiki Komiya, Yoichi Ando, and D. N. Basov, *Phys. Rev. Lett.* **91**, 167401 (2003).
- [93] A. Lanzara, P. V. Bogdanov, X. J. Zhou, S. A. Kellar, D. L. Feng, E. D. Lu, T. Yoshida, H. Eisaki, A. Fujimori, K. Kishio, J.-I. Shimoyama, T. Noda, S. Uchida, Z. Hussain, and Z.-X. Shen, *Nature* **412**, 510 (2001).
- [94] P. D. Johnson, T. Valla, A. V. Fedorov, Z. Yusof, B. O. Wells, Q. Li, A. R. Moodenbaugh, G. D. Gu, N. Koshizuka, C. Kendziora, Sha Jian, and D. G. Hinks, *Phys. Rev. Lett.* **87**, 177007 (2001).
- [95] N. P. Armitage, D. H. Lu, C. Kim, A. Damascelli, K. M. Shen, F. Ronning, D. L. Feng, P. Bogdanov, X. J. Zhou, W. L. Yang, Z. Hussain, P. K. Mang, N. Kaneko, M. Greven, Y. nose, Y. Taguchi, Y. Tokura, and Z.-X. Shen, *Phys. Rev. B* **68**, 064517 (2003).
- [96] A. D. Gromko, A. V. Fedorov, Y.-D. Chuang, J. D. Koralek, Y. Aiura, Y. Yamaguchi, K. Oka, Yoichi Ando, and D. S. Dessau, *Phys. Rev. B* **68**, 174520 (2003).
- [97] T. Sato, H. Matsui, T. Takahashi, H. Ding, H.-B. Yang, S.-C. Wang, T. Fujii, T. Watanabe, A. Matsuda, T. Terashima, and K. Kadowaki, *Phys. Rev. Lett.* **91**, 157003 (2003).
- [98] Ch. Renner, B. Revaz, J.-Y. Genoud, K. Kadowaki, and O. Fischer, *Phys. Rev. Lett.* **80**, 149 (1998); M. Suzuki, and T. Watanabe, *Phys. Rev. Lett.* **85**, 4787 (2000).
- [99] M. Kugler, O. Fischer, Ch. Renner, S. Ono, and Yoichi Ando, *Phys. Rev. Lett.* **86**, 4911 (2001); A. Yurgens, D. Winkler, T. Claeson, S. Ono, and Yoichi Ando, *Phys. Rev. Lett.* **90**, 147005 (2003).
- [100] D. L. Feng, N. P. Armitage, D. H. Lu, A. Damascelli, J. P. Hu, P. Bogdanov, A. Lanzara, F. Ronning, K. M. Shen, H. Eisaki, C. Kim, and Z.-X. Shen, *Phys. Rev. Lett.* **86**, 5550 (2001).
- [101] S. V. Borisenko, A. A. Kordyuk, T. K. Kim, A. Koitzsch, M. Knupfer, J. Fink, M. S. Golden, M. Eschrig, H. Berger, and R. Follath, *Phys. Rev. Lett.* **90**, 207001 (2003); T. K. Kim, A. A. Kordyuk, S. V. Borisenko, A. Koitzsch, M. Knupfer, H. Berger, and J. Fink, *Phys. Rev. Lett.* **91**, 167002 (2003).
- [102] C. Janowitz, R. Mueller, L. Dudy, A. Krampf, R. Manzke, C. Ast, and H. Hoehst, *Europhys. Lett.* **60**, 615 (2002).
- [103] M. Plate, J. D. F. Mottershead, I. S. Elfimov, D. C. Peets, Ruixing Liang, D. A. Bonn, W. N. Hardy, S. Chiuzaian, M. Falub, M. Shi, L. Patthey, and A. Damascelli, <http://aps.arxiv.org/abs/cond-mat/0503117>.
- [104] D. S. Marshall, D. S. Dessau, A. G. Loeser, C.-H. Park, A. Y. Matsuura, J. N. Eckstein, I. Bozovic, P. Fournier, A. Kapitulnik, W. E. Spicer, and Z.-X. Shen, *Phys. Rev. Lett.* **76**, 4841 (1996).
- [105] M. R. Norman, H. Ding, M. Randeria, J. C. Campuzano, T. Yokoya, T. Takeuchi, T. Takahashi, T. Mochiku, K. Kadowaki, P. Guptasarma, and D. G. Hinks, *Nature* **392**, 157 (1998).
- [106] T. Yoshida, X. J. Zhou, T. Sasagawa, W. L. Yang, P. V. Bogdanov, A. Lanzara, Z. Hussain, T. Mizokawa, A. Fujimori, H. Eisaki, Z.-X. Shen, T. Kakeshita, and S. Uchida, *Phys. Rev. Lett.* **91**, 027001 (2003).
- [107] K. M. Shen, T. Yoshida, D. H. Lu, F. Ronning, N. P. Armitage, W. S. Lee, X. J. Zhou, A. Damascelli, D. L. Feng, N. J. C. Ingle, H. Eisaki, Y. Kohsaka, H. Takagi, T. Kakeshita, S. Uchida, P. K. Mang, M. Greven, Y. Onose, Y. Taguchi, Y. Tokura, Seiki Komiya, Yoichi Ando, M. Azuma, M. Takano, A. Fujimori, and Z.-X. Shen, *Phys. Rev. B* **69**, 054503 (2004).
- [108] Yoichi Ando, A. N. Lavrov, Seiki Komiya, Kouji Segawa, and X. F. Sun, *Phys. Rev. Lett.* **87**, 017001 (2001).
- [109] J. F. Zasadzinski, L. Ozyuzer, N. Miyakawa, K. E. Gray, D. G. Hinks, and C. Kendziora, *Phys. Rev. Lett.* **87**, 067005 (2001).

- [110] Ph. Bourges, Y. Sidis, H. F. Fong, L. P. Regnault, J. Bossy, A. Ivanov, and B. Keimer, *Science* **288**, 1234 (2000); Ph. Bourges, B. Keimer, S. Pailhès, L. P. Regnault, Y. Sidis, and C. Ulrich, <http://aps.arxiv.org/abs/cond-mat/0211227>; Y. Sidis, S. Pailhès, B. Keimer, P. Bourges, C. Ulrich, and L. P. Regnault, *Phys. Stat. Sol. (b)* **241**, 1204 (2004).
- [111] D. Reznik, P. Bourges, L. Pintschovius, Y. Endoh, Y. Sidis, T. Matsui, and S. Tajima, *Phys. Rev. Lett.* **93**, 207003 (2004).
- [112] J. M. Tranquada, H. Woo, T. G. Perring, H. Goka, G. D. Gu, G. Xu, M. Fujita, and K. Yamada, *Nature* **429**, 534 (2004).
- [113] S. M. Hayden, H. A. Mook, Pengcheng Dai, T. G. Perring, and F. Dogan, *Nature* **429**, 531 (2004).
- [114] C. Stock, W. J. L. Buyers, R. A. Cowley, P. S. Clegg, R. Coldea, C. D. Frost, R. Liang, D. Peets, D. Bonn, W. N. Hardy, and R. J. Birgeneau, *Phys. Rev. B* **71**, 024522 (2005).
- [115] J. M. Tranquada, C. H. Lee, K. Yamada, Y. S. Lee, L. P. Regnault, and H. M. Ronnow, *Phys. Rev. B* **69**, 174507 (2004).
- [116] S. Wakimoto, H. Zhang, K. Yamada, I. Swainson, Hyunkyung Kim, and R. J. Birgeneau, *Phys. Rev. Lett.* **92**, 217004 (2004).
- [117] N. B. Christensen, D. F. McMorrow, H. M. Ronnow, B. Lake, S. M. Hayden, G. Aeppli, T. G. Perring, M. Mangkorntong, M. Nohara, and H. Takagi, *Phys. Rev. Lett.* **93**, 147002 (2004).
- [118] D. L. Feng, D. H. Lu, K. M. Shen, C. Kim, H. Eisaki, A. Damascelli, R. Yoshizaki, J.-i. Shimoyama, K. Kishio, G. D. Gu, S. Oh, A. Andrus, J. O'Donnell, J. N. Eckstein, and Z.-X. Shen, *Science* **289**, 277 (2000); H. Ding, J. R. Engelbrecht, Z. Wang, J. C. Campuzano, S.-C. Wang, H.-B. Yang, R. Rogan, T. Takahashi, K. Kadowaki, and D. G. Hinks, *Phys. Rev. Lett.* **87**, 227001 (2001).
- [119] R. H. He, D. L. Feng, H. Eisaki, J.-I. Shimoyama, K. Kishio, and G. D. Gu, *Phys. Rev. B* **69**, 220502 (2004).
- [120] P. W. Anderson, and N. P. Ong, <http://aps.arxiv.org/abs/cond-mat/0405518>.
- [121] S. Kashiwaya, T. Ito, K. Oka, S. Ueno, H. Takashima, M. Koyanagi, Y. Tanaka, and K. Kajimura, *Phys. Rev. B* **57**, 8680 (1998).
- [122] C.-T. Chen, P. Seneor, N.-C. Yeh, R. P. Vasquez, L. D. Bell, C. U. Jung, J. Y. Kim, Min-Seok Park, Heon-Jung Kim, and Sung-Ik Lee, *Phys. Rev. Lett.* **88**, 227002 (2002).
- [123] B. Fisher, J. Genossar, I. O. Lelong, A. Kessel, and J. Ashkenazi, *J. Supercond.* **1**, 53 (1988); J. Genossar, B. Fisher, I. O. Lelong, J. Ashkenazi, and L. Patlagan, *Physica C* **157**, 320 (1989).
- [124] S. Bar-Ad, B. Fisher, J. Ashkenazi, and J. Genossar, *Physica C* **156**, 741 (1988).
- [125] S. Tanaka, M. Sera, M. Sato, and H. Fujishita, *J. Phys. Soc. Japan* **61**, 1271 (1992); K. Matsuura, T. Wada, Y. Yaegashi, S. Tajima, and H. Yamauchi, *Phys. Rev. B* **46**, 11923 (1992); S. D. Obertelli, J. R. Cooper, and J. L. Tallon, *Phys. Rev. B* **46**, 14928 (1992); C. K. Subramaniam, A. B. Kaiser, H. J. Trodahl, A. Mawdsley, and R. G. Buckley, *Physica C* **203**, 298 (1992).
- [126] Y. Kubo and T. Manako, *Physica C* **197**, 378 (1992).
- [127] H. Y. Hwang, B. Batlogg, H. Takagi, H. L. Kao, J. Kwo, R. J. Cava, J. J. Krajewski, and W. F. Peck, Jr., *Phys. Rev. Lett.* **72**, 2636 (1994).
- [128] Seongshik Oh, Tiziana Di Luccio, and J. N. Eckstein, *Phys. Rev. B* **71**, 052504 (2005).
- [129] J. Takeda, T. Nishikawa, and M. Sato, *Physica C* **231**, 293 (1994); X.-Q. Xu, S. J. Hagen, W. Jiang, J. L. Peng, Z. Y. Li, and R. L. Greene, *Phys. Rev. B* **45**, 7356 (1992); Wu Jiang, S. N. Mao, X. X. Xi, Xiuguang Jiang, J. L. Peng, T. Venkatesan, C. J. Lobb, and R. L. Greene, *Phys. Rev. Lett.* **73**, 1291 (1994).
- [130] G. V. M. Williams, R. Dupree, A. Howes, S. Krämer, H. J. Trodahl, C. U. Jung, Min-Seok Park, and Sung-Ik Lee, *Phys. Rev. B* **65**, 224520 (2002).
- [131] N. P. Armitage, F. Ronning, D. H. Lu, C. Kim, A. Damascelli, K. M. Shen, D. L. Feng, H. Eisaki, Z.-X. Shen, P. K. Mang, N. Kaneko, M. Greven, Y. Onose, Y. Taguchi, and Y. Tokura, *Phys. Rev. Lett.* **88**, 257001 (2002).
- [132] P. G. Steeneken, L. H. Tjeng, G. A. Sawatzky, A. Tanaka, O. Tjernberg, G. Ghiringhelli, N. B. Brookes, A. A. Nugroho, and A. A. Menovsky, *Phys. Rev. Lett.* **90**, 247005 (2003).
- [133] A. V. Boris, N. N. Kovaleva, O. V. Dolgov, T. Holden, C. T. Lin, B. Keimer, and C. Bernhard, *Science* **304**, 708 (2004); A. F. Santander-Syro, and N. Bonetemp, <http://aps.arxiv.org/abs/cond-mat/0503767>; A. B. Kuzmenko, H. J. A. Molegraaf, F. Carbone, and D. van der Marel, <http://aps.arxiv.org/abs/cond-mat/0503768>.
- [134] W. Kohn and L. J. Sham, *Phys. Rev.* **140**, A1133 (1965).
- [135] W. J. Padilla, M. Dumm, Seiki Komiya, Yoichi Ando, and D. N. Basov, <http://aps.arxiv.org/abs/cond-mat/0505094>.
- [136] Y.-S. Lee, Kouji Segawa, Yoichi Ando, and D. N. Basov, *Phys. Rev. B* **70**, 014518 (2004).
- [137] C. C. Homes, S. V. Dordevic, D. A. Bonn, R. Liang, W. N. Hardy, and T. Timusk, *Phys. Rev. B* **71**, 184515 (2005).
- [138] T. Shibauchi, H. Kitano, K. Uchinokura, A. Maeda, T. Kimura and K. Kishio, *Phys. Rev. Lett.* **72**, 2263 (1994).
- [139] D. N. Basov, T. Timusk, B. Dabrowski, and J. D. Jorgensen, *Phys. Rev. B* **50**, 3511 (1994).
- [140] D. N. Basov, H. A. Mook, B. Dabrowski, and T. Timusk, *Phys. Rev. B* **52**, R13141 (1995).
- [141] Vinay Ambegaokar and Alexis Baratoff, *Phys. Rev. Lett.* **10**, 486 (1963).
- [142] W. E. Lawrence, and S. Doniach, in *Proceedings of the Twelfth International Conference on Low Temperature Physics*, edited by E. Kanda, (Academic Press of Japan, Kyoto 1971), p. 361.
- [143] Diana Dulic, D. van der Marel, A. A. Tsvetkov, W. N. Hardy, Z. F. Ren, J. H. Wang, and B. A. Willemssen, *Phys. Rev. B* **60**, R15051 (1999).
- [144] S. V. Dordevic, Seiki Komiya, Yoichi Ando, and D. N. Basov, *Phys. Rev. Lett.* **91**, 167401 (2003).
- [145] A. J. Leggett, *Prog. Theor. Phys.* **36**, 901 (1966).
- [146] C. C. Homes, S. V. Dordevic, T. Valla, and M. Strongin, <http://aps.arxiv.org/abs/cond-mat/0410719>.
- [147] M. S. Osofsky, R. J. Soulen, Jr., J. H. Claassen, G. Trotter, H. Kim, and J. Horwitz, *Phys. Rev. B* **66**, 020502 (2002).